ER to Golgi Transport: Requirement for p115 at a Pre-Golgi VTC Stage

Cecilia Alvarez,* Hideaki Fujita,‡ Ann Hubbard,‡ and Elizabeth Sztul*

*Department of Cell Biology, University of Alabama at Birmingham, Birmingham, Alabama 35294; and ‡Department of Cell Biology and Anatomy, Johns Hopkins University School of Medicine, Baltimore, Maryland 21205

Abstract. The membrane transport factor p115 functions in the secretory pathway of mammalian cells. Using biochemical and morphological approaches, we show that p115 participates in the assembly and maintenance of normal Golgi structure and is required for ER to Golgi traffic at a pre-Golgi stage. Injection of antibodies against p115 into intact WIF-B cells caused Golgi disruption and inhibited Golgi complex reassembly after BFA treatment and wash-out. Addition of anti–p115 antibodies or depletion of p115 from a VSVtsO45 based semi-intact cell transport assay inhibited transport. The inhibition occurred after VSV glycoprotein (VSV-G) exit from the ER but before its delivery to the Golgi complex, and resulted in VSV-G protein accumulating in peripheral vesicular tubular clusters (VTCs). The p115-requiring step of transport followed the rab1-requiring step and preceded the Ca^{2+}-requiring step. Unexpectedly, mannosidase I redistributed from the Golgi complex to colocalize with VSV-G protein arrested in pre-Golgi VTCs by p115 depletion. Redistribution of mannosidase I was also observed in cells incubated at 15°C. Our data show that p115 is essential for the translocation of pre-Golgi VTCs from peripheral sites to the Golgi stack. This defines a previously uncharacterized function for p115 at the VTC stage of ER to Golgi traffic.

Key words: VTCs • Golgi complex • p115 • ER–Golgi transport

ENDOPLASMIC reticulum (ER) to Golgi traffic has been extensively studied and a general framework for the process has been elucidated (for reviews see Bannykh et al., 1998; Hong, 1998; Glick and Malhotra, 1998). Export from the ER defines the first step of the pathway and is mediated by the recruitment of the coat protein (COP)[1] II coats (composed of sec23/24 and sec13/31 complexes and Sar1p) and the subsequent budding of COP II–coated vesicles (for review see Barlowe, 1998). The coat proteins direct the sorting and concentration of proteins into the budding profiles, resulting in the preferential recruitment of cargo and exclusion of resident ER proteins (Aridor et al., 1998). COP II vesicles bud from specialized ER export sites morphologically defined as an assembly of centrally located tubules surrounded by budding profiles still attached to the ER (Bannykh et al., 1996; Bannykh and Balch, 1997). Budded COP II vesicles fuse with each other and with already fused vesicles to form the polymorphic tubular structures that have been called ERGIC (ER–Golgi intermediate compartment), intermediate compartment, or vesicular tubular clusters (VTCs) (Saraste and Svensson, 1991; Balch et al., 1994; Tang et al., 1995; Bannykh et al., 1998). VTCs comprise a morphologically and functionally complex compartment integrating the anterograde ER to Golgi complex and the retrograde recycling transport pathways. VTCs progress from the cell periphery towards the microtubule organizing center and the adjoining Golgi complex on microtubules in a dynein/dynactin–mediated process (for review see Lippincott-Schwartz, 1998). During their limited life span, VTCs undergo maturation by the selective recycling and acquisition of specific proteins and the sequential exchange of specific molecules (e.g., COP II coats exchange for COP I coats on VTCs [Pepperkok et al., 1993; Peter et al., 1993; Aridor et al., 1995; Scales et al., 1997]). Current evidence favors the view that COP I vesicles mediate the selective retrieval of proteins from the Golgi back to the VTCs and/or the ER, but their participation in anterograde traffic has not been ruled out (Lowe and Kreis, 1998). VTCs accumulate in the peri-Golgi region and, once there, seem to form a more extensive array of tubules, sometimes called the cis-Golgi network or the

Address correspondence to Elizabeth Sztul, Department of Cell Biology, University of Alabama at Birmingham, McCallum Building, Birmingham, AL 35294. Tel.: (205) 934-1465. Fax: (205) 975-9131. E-mail: esztul@uab.edu

1. *Abbreviations used in this paper:* BFA, brefeldin A; COP, coat protein; endo-D, endoglycosidase D; endo-H, endoglycosidase H; ERGIC, ER–Golgi intermediate compartment; Mann I/II, mannosidase I and II, respectively; NAGT-1, *N*-acetylglucosamine transferase I; NRK, normal rat kidney; SNAP, soluble NSF attachment protein; v- and t-SNARES, vesicle- and target-SNAP receptors; VSV, vesicular stomatitis virus; VSV-G, VSV glycoprotein; VSVtsO45, temperature-sensitive strain of VSV; VTCs, vesicular tubular clusters.

CGN. The exact relationship between VTCs and the CGN is unclear and it is possible that VTCs fuse to make a CGN or that the CGN is a large aggregate of individual VTCs.

Fusion of COP II vesicles to form VTCs and the subsequent assembly of VTCs to form cis-Golgi requires the concerted function of numerous molecules, among them the compartment-specific GTPases rab1 (Plutner et al., 1991; Tisdale et al., 1992; Pind et al., 1994) and rab2 (Chavrier et al., 1990; Tisdale et al., 1992; Tisdale and Balch, 1996), the general soluble fusion factors NSF (*N*-ethylmaleimide–sensitive fusion factor) and SNAP (soluble NSF attachment protein), and a set of distinct integral membrane proteins v-SNARES and t-SNARES (vesicle- and target-SNAP receptors) believed to confer specificity to fusion (Söllner et al., 1993; for reviews see Rothman, 1994; Hay and Scheller, 1997; Nichols and Pelham, 1998). The molecular mechanism underlying membrane traffic is highly conserved, and in yeast, ER to Golgi transport is also dependent on the function of the compartment-specific GTPase Ypt1p (Segev et al., 1988), the general fusion factors Sec18p (NSF homologue) and Sec17p (SNAP homologue), and the specific interactions of ER–Golgi SNAREs (Bos1p, Bet1p, Sed5p, Sec22p, and Ykt6p) (for reviews see Ferro-Novick and Jahn, 1994; McNew et al., 1997). SNAREs mediate membrane interactions at relatively short distances (an assembled SNARE pair has been shown to be only 14 nm; Hanson et al., 1997), and it appears that donor and target membranes interact at longer distances through the selective interactions of specific tethering proteins (Orci et al., 1998; for review see Pfeffer, 1996). In yeast, tethering of COP II vesicles to Golgi membranes (yeast do not have morphologically identifiable VTCs) occurs before SNARE complex formation and is dependent on the function of a peripheral membrane–associated protein, Uso1p (Nakajima et al., 1991; Sapperstein et al., 1996; Cao et al., 1998).

A mammalian homologue of Uso1p, p115, has been characterized and shown to have a multidomain structure composed of an NH_2-terminal globular head, central coiled-coil region, and a COOH-terminal acidic domain (Barroso et al., 1995; Sapperstein et al., 1995; Yamakawa et al., 1996). Like Uso1p, p115 assembles into parallel dimers. Functionally, p115 has been identified as a requirement in in vivo–reconstituted assays measuring cis- to medial-Golgi transport (Waters et al., 1992), transcytotic traffic (Barroso et al., 1995), regrowth of Golgi cisterna from mitotic Golgi fragments (Rabouille et al., 1995, 1998; Nakamura et al., 1997), and cisternal stacking (Shorter and Warren, 1999). Consistent with the role of p115 in Golgi events, p115 has been localized predominantly to the Golgi at the light microscope level. However, by electron microscopy, p115 was found preferentially associated with VTCs adjacent to the Golgi stack (the close proximity of VTCs to the Golgi [Ladinsky et al., 1999] makes them difficult to resolve from Golgi elements by immunofluorescence), and to cycle extensively between the Golgi and earlier compartments of the secretory pathway (Nelson et al., 1998). Such localization and cycling behavior is characteristic for proteins involved in ER to Golgi traffic, suggesting that p115, like Uso1p, might participate in this stage of the secretory pathway.

Here, we show that p115 is critical for the dynamic maintenance and the de novo assembly of morphologically normal Golgi complexes, and that p115 is required for ER to Golgi traffic at a pre-Golgi VTC stage, after the rab1-requiring step but preceding the Ca^{2+}-requiring step. Biochemical and morphological analysis of cargo VSV glycoprotein (VSV-G) protein progression from the ER to the Golgi indicated that p115 function is not essential for events leading to the formation of VTCs, but that p115 is required for the subsequent delivery of VTCs from the peripheral sites, where they form, to the Golgi stack. Characterization of the p115-arrested VTCs showed that the cis-Golgi enzyme mannosidase I (Mann I), but not Mann II, specifically redistributed from the Golgi stack and colocalized with such VTCs. Our results indicate that p115 is required for traffic progression along the secretory pathway at a pre-Golgi VTC step, suggesting that p115 is essential for events leading to VTC delivery to the Golgi stack.

Materials and Methods

Antibodies

Rabbit polyclonal antibodies against p115 were generated by immunization with purified rat p115 (Barroso et al., 1995). For affinity purification of antibodies, purified GST-p115 fusion protein was run on 7.5% acrylamide gels, and transferred to nitrocellulose. Strips of nitrocellulose containing p115 were incubated with immune serum in PBS, 5% dried milk, and 0.1% Tween 20 for 3 h at room temperature. Bound antibodies were eluted with 0.1 M glycine, pH 3.0, and then neutralized with 1/10 vol 1 M phosphate buffer, pH 7.4. These anti–p115 antibodies were either used in transport assays or cross-linked to protein A–Sepharose 4 FF (Pharmacia Biotech, Inc.) with dimethyl pimelimidate (Pierce Chemical Co.) according to the manufacturer's protocol, and subsequently used for p115 immunodepletion experiments. Mouse polyclonal antibodies against GM130 were generated by immunization with inclusion bodies from bacteria expressing full-length GM130 (Nelson et al., 1998). Anti-giantin monoclonal G1/133 (Linstedt and Hauri, 1993) and anti–ERGIC-53 monoclonal G1/93 (Schweizer et al., 1988) were provided by Dr. Hans-Peter Hauri (University of Basel, Basel, Switzerland). Polyclonal antibodies against Mann II were kindly provided by Dr. Marilyn Farquhar (University of California, San Diego, CA). mAbs against Mann II were from Sigma Chemical Co. Anti–rab1 antibodies were a gift of Dr. Mark McNiven (Mayo Foundation, Rochester, MN). Polyclonal antibodies against Mann I were provided by Dr. Kelley Moreman (University of Georgia, Athens, GA). Monoclonal anti–VSV-G protein (P5D4) was provided by Dr. Kathryn Howell (University of Colorado, Denver, CO). Goat anti–rat and anti–mouse antibodies conjugated with FITC or rhodamine were purchased from Jackson ImmunoResearch.

Generation of GST-p115 Construct

Full-length p115 was cloned into the BamHI-NotI restriction sites of the pGEX-6P-2 GST vector (Pharmacia Biotech, Inc.). p115 was obtained by PCR using as a template a pBluescript-II-KS plasmid (Stratagene) encoding rat p115 cDNA previously described (Barroso et al., 1995). GST-p115 fusion protein expression and purification were performed according to the manufacturer's protocol.

Purification of Cytosolic p115

p115 was affinity-purified from rat liver cytosol using affinity-purified polyclonal antibodies raised against p115 cross-linked to beads as previously described (Barroso et al., 1995). The p115 preparation was judged homogenous by Coomassie blue staining.

Microinjection

Ascites raised against p115 (3A10) were concentrated by centrifugation in a Microcon 30 (Pierce Chemical Co.) and dialyzed into MI buffer (48 mM K_2HPO_4, 140 mM NaH_2PO_4, 4.5 mM KH_2PO_4, pH 7.2). Denaturation was by boiling to 100°C for 3 min. Before injection, solutions were centrifuged

at 15,800 *g* for 20 min, and then mixed with 1/10 vol of Texas red–dextran (TR-dextran, 10,000 D, 50 mg/ml) and 10× MI buffer. Injections into the cytoplasm of WIF-B cells were performed with an Eppendorf transjector 5246 and micromanipulator 5171 attached to a Zeiss Axiovert 100 microscope. The pressure was 50 hectoPascal for 0.1–0.2 s using an Eppendorf femtotip needle. After injection, cells were incubated with Ham's F12 medium (Gibco Laboratories) at 37°C for 2–3 h, fixed, and processed for immunofluorescence. In some experiments, 2.5 μg/ml BFA was used. Fluorescent images were collected with the MCID analysis system (Zeiss Axiovert 100 microscope) or with a Zeiss confocal microscope (LSM410). Digitized images were cropped, assembled, and labeled in Adobe Photoshop.

Semi-intact Cell ER–Golgi Transport Assay

The ER to Golgi transport assay was performed as described previously (Beckers et al., 1987; Schwaninger et al., 1992b). In brief, normal rat kidney (NRK) cells, or LEC-1 (a CHO-derived cell line deficient in NAGT-1 and analogous to CHO15B) cells were grown on 10-cm petri dishes to 80–90% of confluence and infected with the temperature-sensitive strain of the vesicular stomatitis virus, VSVtsO45 at 32°C for 3–4 h (Bergmann, 1989). The cells were pulse-labeled with ^{35}S-trans label (200 mCi/ml; ICN) at the restrictive temperature (42°C) for 10 min, chased with complete medium for 5 min, and perforated by hypotonic swelling and scraping to make semi-intact cells. A transport reaction was performed in a final total volume of 40 μl in a buffer that contained 25 mM Hepes-KOH, pH 7.2, 75 mM potassium acetate, 2.5 mM magnesium acetate, 5 mM EGTA, 1.8 mM $CaCl_2$, 1 mM *N*-acetylglucosamine, ATP regeneration system (1 mM ATP, 5 mM creatine phosphate, and 0.2 IU rabbit muscle creatine phosphokinase), 5 μl rat liver cytosol, 5 μl of semi-intact cells in 50 mM Hepes-KOH, pH 7.2, and 90 mM potassium acetate. Transport was initiated by transfer of cells to 32°C. After 90 min of incubation, cells were pelleted, resuspended in appropriated buffer, and digested with endoglycosidase H (endo-H) or endoglycosidase D (endo-D) as described previously (Schwaninger et al., 1992b). The samples were analyzed on 8% SDS-PAGE and fluorography. The transport was quantified using GS-700 imaging densitometer (Bio-Rad Laboratories). For antibody inhibition of transport assay, affinity-purified p115 antibodies were added into the complete assay cocktail and incubated on ice for 30 min before use. Staging experiments were performed as previously described (Peter et al., 1998).

Immunodepletion of Rat Liver Cytosol

Rat liver cytosol was prepared as previously described (Dascher et al., 1994). Immunopurified anti–p115 antibodies cross-linked to protein A–Sepharose were incubated (2 h at 4°C) with rat liver cytosol, and the level of p115 depletion was tested by SDS-PAGE and immunoblotting.

Morphological Analysis of VSVtsO45 G Protein Transport

This analysis was performed as described previously (Plutner et al., 1992). In brief, NRK cells plated on coverslips were infected with VSVtsO45 at 32°C for 30 min, followed by an incubation at 42°C for 3 h, and then shifted to ice and permeabilized with digitonin (20 mg/ml). Coverslips were incubated in various transport cocktails at 32°C for 90 min. For antibody inhibition of the transport assay, affinity-purified p115 antibodies were added into the complete transport mix and incubated on ice for 30 min followed by an incubation at 32°C for 90 min. Transport was determined by transferring coverslips to ice and fixing them in 3% formaldehyde/PBS for 10 min. The coverslips were processed for double label immunofluorescence.

Immunofluorescence Microscopy

Cells grown on glass coverslips were washed three times in PBS and fixed in 3% paraformaldehyde in PBS for 10 min at room temperature. Paraformaldehyde was quenched with 10 mM ammonium chloride, and cells were permeabilized with PBS, 0.1% Triton X-100 for 7 min at room temperature. The coverslips were washed (three times, 2 min per wash) with PBS, and blocked in PBS, 0.4% fish skin gelatin, 0.2% Tween 20 for 5 min, followed by blocking in PBS, 2.5% goat serum, 0.2% Tween for 5 min. Cells were incubated with primary antibody diluted in PBS, 0.4% fish skin gelatin, and 0.2% Tween 20 for 45 min at 37°C. Coverslips were washed (five times, 5 min per wash) with PBS and 0.2% Tween 20. Secondary antibodies coupled to FITC or rhodamine were diluted in 2.5% goat serum and incubated on coverslips for 30 min at 37°C. Coverslips were washed with PBS and 0.2% Tween 20 as above, and mounted on slides in 9:1 glycerol/PBS with 0.1% q-phenylenediamine. Fluorescence patterns were visualized with an Olympus IX70 epifluorescence microscope. Optical sections were captured with a CCD high resolution camera equipped with a camera/computer interface. Images were analyzed with a power Mac 9500/132 computer using IPLab Spectrum software (Scanalytics Inc.).

Results

Antibodies against p115 Disrupt Golgi Structure and Prevent Reassembly of Golgi Stacks In Vivo

The requirement for p115 has been previously studied only in in vitro–reconstituted assays (Waters et al., 1992; Barroso et al., 1995; Rabouille et al., 1995, 1998). To examine the function of p115 in vivo, monoclonal anti–p115 an-

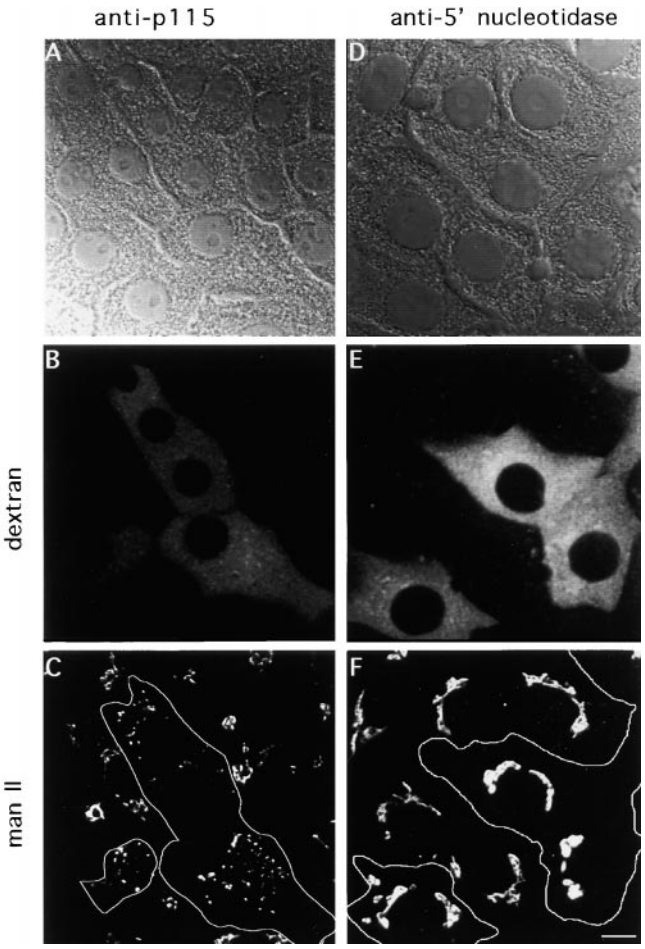

Figure 1. Antibodies against p115 cause Golgi complex disassembly. mAbs against p115 mixed with TR-dextran (A–C), or mAbs against 5′-nucleotidase mixed with TR-dextran (D–F) were microinjected into the cytoplasm of WIF-B cells. Phase images of cells are shown (A and D). Injected cells are identified by TR-dextran (B and E) and are traced in outline in C and F. Cells were fixed 2 h after injection and processed for immunofluorescence using antibodies against Mann II (C and F). Cells injected with anti–p115 antibodies, but not uninjected cells or cells injected with control antibodies show disassembly of Golgi complexes. Bar, 10 μm.

tibodies were microinjected into WIF-B cells (Shanks et al., 1994), and their effect on Golgi structure was monitored by the distribution of Mann II. As shown in Fig. 1, injection of anti–p115 antibodies had an effect on Golgi structure. A field of cells is shown by phase-contrast (A), and the injected cells are identified by their content of coinjected TR-dextran (B). Within 2 h after injection, the Golgi complexes in all injected cells were disassembled, and Mann II was present in relatively large punctate structures dispersed throughout the cells (C). The structures appeared superficially similar to those observed in cells transfected with mutant forms of p115 lacking portions of the globular head or the coiled-coil tail (Nelson et al., 1998). Injection of control antibodies against the bile canalicular plasma membrane protein 5′-nucleotidase did not perturb Golgi structure (D–F).

ER to Golgi traffic can be disrupted by brefeldin A (BFA), which inhibits a guanine nucleotide exchange factor for ADP ribosylation factor; thus, preventing assembly of COP I coats, and ultimately blocking normal traffic between ER and the Golgi (Donaldson et al., 1992b; Helms and Rothman, 1992). This results in COP I–independent tubulation of the Golgi and the relocation of Golgi proteins into the ER (Misumi et al., 1986; Fujiwara et al., 1988; Lippincott-Schwartz et al., 1989). BFA-induced membrane redistribution has given valuable insights into components and mechanisms involved in regulation of the secretory pathway (Klausner et al., 1992), and we combined BFA treatments with microinjection of anti–p115 antibodies to characterize the effect of anti–p115 antibodies on ER–Golgi traffic.

The redistribution of Mann II from the Golgi into the ER in control WIF-B cells or in cells injected with anti–p115 antibodies was examined first. As shown in Fig. 2, Mann II was detected in a normal perinuclear Golgi pattern in uninjected cells or in injected cells immediately after the antibody injection and before BFA treatment (A). The injected cells were identified by the presence of anti–p115 IgG (B). When an analogous field of cells was treated with BFA for 30 min, Mann II relocated from the Golgi to the ER in uninjected and injected cells (C). Only a single time point was analyzed, and it remains possible that the kinetics of Mann II redistribution may have varied in injected and uninjected cells. Some Golgi staining was still evident in uninjected and injected cells after the BFA treatment (C, arrowheads). After 30 min, the majority of anti–p115 IgG was associated with membranes, presumably representing p115 localization (D), as shown previously (Nelson et al., 1998). The results suggest that anti–p115 antibodies do not block the Golgi to ER redistribution of Mann II induced by BFA treatment.

To examine if the antibodies inhibit the movement of Mann II from the ER, WIF-B cells were first treated with BFA for 30 min to relocate Mann II from the Golgi to the ER, and then injected with anti–p115 antibodies. The temporal sequence of Golgi recovery after BFA wash-out was followed. As shown in Fig. 3 A, punctate structures dispersed throughout the cell were detected after a 10-min BFA wash-out in both, uninjected and injected cells. The size and distribution of the elements were comparable, suggesting that the antibodies do not block early stages of BFA recovery. A difference was seen after 30 min of BFA

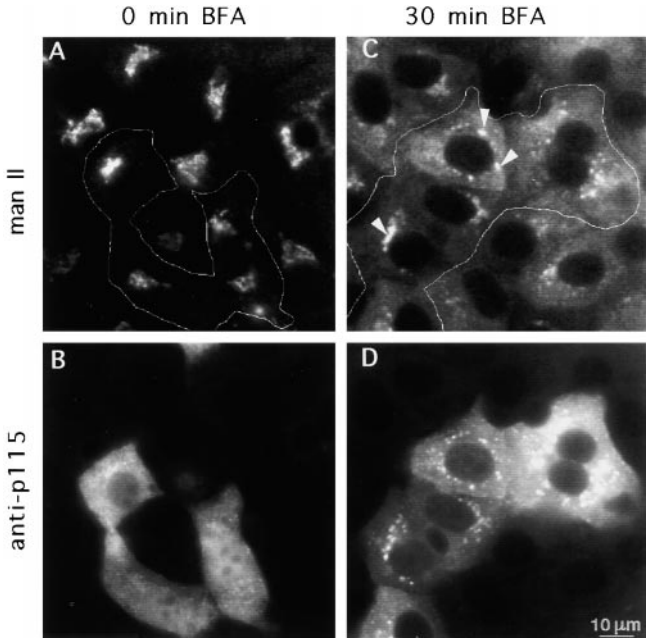

Figure 2. Antibodies against p115 do not block BFA-induced retrograde Golgi to ER traffic. Mouse mAbs against p115 were microinjected into the cytoplasm of WIF-B cells. Cells were fixed immediately after injection (A and B) or after a 30-min BFA treatment (C and D). Cell were processed for double label immunofluorescence using antibodies against Mann II (A and C) or against mouse IgG (B and D). Relocation of Mann II from the Golgi to the ER appears indistinguishable in injected and uninjected cells. Golgi remnants were detected in some cells after the 30-min BFA treatment (C, arrowheads).

wash-out, when defined Golgi structures could be seen in uninjected cells (C, arrows), while significantly smaller, dispersed structures were present in the injected cells (C, arrowheads). The effect was also evident after 120 min of BFA wash-out, when compact Golgi structures were seen in uninjected cells (E, arrows), whereas dispersed punctate structures persisted in the injected cells (E, arrowheads). In some injected cells, a more Golgi-like Mann II pattern was seen (E, asterisk), but the structure appeared less compact and organized. These results suggest that anti–p115 antibodies prevent the reassembly of normal Golgi complexes.

p115 Is Associated with Functional VTCs Moving VSV-G Protein from the ER to the Golgi

The inhibitory effects of anti–p115 antibodies on the maintenance and reassembly of normal Golgi structure, coupled with the previous finding that p115 is present on VTCs and cycles between the Golgi and earlier secretory compartments (Nelson et al., 1998), suggested a potential role for p115 in ER to Golgi transport. To analyze if p115 is present on functional VTCs transporting cargo from the ER to the Golgi, we used a temperature-sensitive strain of the vesicular stomatitis virus (VSVtsO45) as a transport marker (for review see Bergmann, 1989). The viral VSV-G protein fails to exit the ER at 42°C, the nonpermissive temperature, but after shifting the cells to the permissive temperature of 32°C, a wave of VSV-G protein enters the

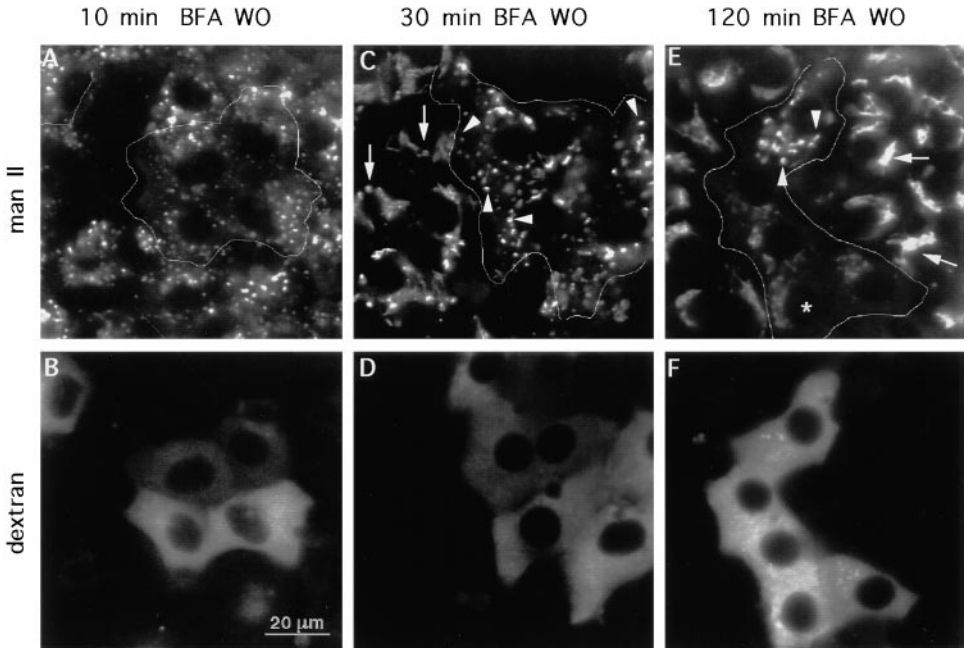

Figure 3. Antibodies against p115 block Golgi complex reassembly during BFA wash-out. WIF-B cells were treated with BFA for 30 min, and then injected with mAbs against p115 mixed with TR-dextran. Cells were fixed after 10 min (A and B), 30 min (C and D), or 120 min (E and F) of BFA wash-out, and processed for immunofluorescence using antibodies against Mann II (A, C, and E). Injected cells were identified by their content of TR-dextran (B, D, and F), and are traced in outline in A, C, and E. After 10 min of BFA wash-out, Mann II relocation to punctate structures is indistinguishable in injected and uninjected cells. After 30 and 120 min of BFA wash-out, Mann II appears in morphologically normal Golgi structures in uninjected cells, but remains in punctate structures in injected cells. Arrowheads mark Golgi in injected cells, arrows point to Golgi in uninjected cells. Asterisk denotes a more compact Golgi complex in injected cells.

secretory pathway, and its movement from the ER to the Golgi can be monitored morphologically (Pepperkok et al., 1993; Balch et al., 1994). NRK cells infected with the virus and cultured at the nonpermissive temperature for 3 h contain VSV-G protein in the ER, whereas p115 is predominantly detected in the Golgi region (Fig. 4, A–C). When infected cells were subsequently shifted from 42 to 15°C and incubated at 15°C for 3 h, VSV-G protein movement to the Golgi was arrested in peripheral VTCs that also contained p115 (Fig. 4, D–F). We have shown previously that p115 colocalizes with the VTC marker, ERGIC-53 (Schweizer et al., 1988) when VTCs are preferentially accumulated during low (15°C) temperature incubation (Saraste and Svensson, 1991; Nelson et al., 1998). Bonafide Golgi proteins such as galactosyl-transferase or Mann II do not redistribute to peripheral VTCs after low temperature treatment (Lippincott-Schwartz et al., 1990; Nelson et al., 1998; see Fig. 10 E). When infected cells were shifted from 42 to 32°C for 1 h, VSV-G protein and p115 colocalized in the Golgi (Fig. 4, G–I). These results indicate that p115 is a component of VTCs that move VSV-G protein from the ER to the Golgi, and raise the possibility that p115 could be involved in VTC dynamics.

p115 Is Required for ER to Golgi Transport

Although p115 has been identified as a cis- to medial-Golgi transport factor (Waters et al., 1992), its yeast homologue, Uso1p, has been shown to act in ER to Golgi traffic (Nakajima et al., 1991; Cao et al., 1998). To examine directly p115 participation in ER to Golgi traffic, we used a previously developed semi-intact cell transport assay (Beckers et al., 1987). NRK cells were infected with VSVtsO45 and radiolabeled at 42°C. Cells were permeabilized to remove endogenous cytosol, supplemented with exogenous transport cocktails, and shifted to 32°C to initiate VSV-G protein transport. Delivery of VSV-G protein to the Golgi was assessed by its carbohydrate processing, as defined by endo-H resistance. VSV-G protein oligosaccharide chains are processed during transport by the sequential actions of enzymes localized throughout the Golgi stack. The processing involves the sequential function of Mann I and *N*-acetylglucosamine transferase I (NAGT-1), both considered cis-Golgi enzymes (Schwaninger et al., 1992b), and of Mann II, localized in the medial/trans Golgi stack (Velasco et al., 1993). After processing by Mann I, VSV-G acquires endo-D sensitivity, whereas subsequent processing by NAGT-1 and Mann II confers endo-H resistance. As shown in Fig. 5 A, when complete transport cocktail was added to permeabilized cells, ~50% of VSV-G protein was processed to an endo-H–resistant form (top band, lane 2), and this is set as 100% processing. The percent processing is analogous to the level of processing reported previously (Tisdale and Balch, 1996; Subramanian et al., 1996). In contrast, when transport was analyzed with an ATP-depleting system, VSV-G protein remained sensitive to endo-H (bottom band, lane 1), and this is set as 0% processing. The addition of increasing amounts of affinity-purified anti–p115 antibodies (from 0.1 to 0.8 μg) led to a dose-dependent inhibition of VSV-G protein processing to the endo-H–resistant form (lanes 3–6). To provide quantitative data on VSV-G processing, analogous data from repeated experiments ($n = 3$) were evaluated by densitometry, and the average of relative percent is presented in the accompanying bar graph. The relative processing was reduced by 15% in the presence of 0.1 μg of antibody with >80% inhibition when 0.4 μg of anti–p115 antibodies were

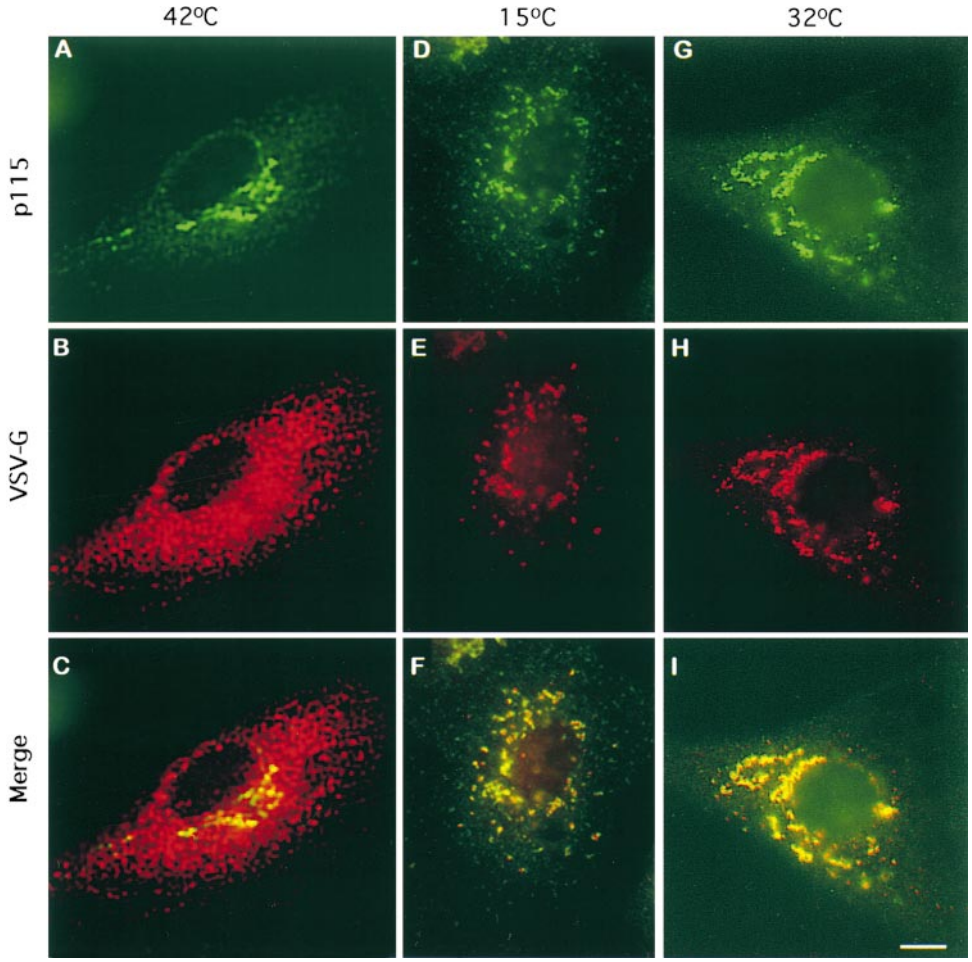

Figure 4. p115 is associated with VTCs moving cargo VSV-G protein from the ER to the Golgi. NRK cells were infected with VSVtsO45 at 42°C for 3 h. The cells were either fixed (A–C) or incubated at 15°C for 3 h (D–F) or at 32°C for 1 h (G–I) before fixation. Cell were processed for double label immunofluorescence using antibodies against p115 (A, D, and G) and antibodies against VSV-G protein (B, E, and H). At 42°C, VSV-G protein is present in the ER (B), whereas p115 is predominantly localized to the Golgi (A). p115 and VSV-G protein colocalize in peripheral VTCs after 15°C incubation (D–F), and in the Golgi after 32°C incubation (G–I). Bar 10 μm.

added. When preimmune antibodies were added to the transport assay, normal processing of VSV-G protein was observed (data not shown).

To ensure that the inhibitory effects of the anti–p115 antibodies were due to an interaction with p115, the antibodies were preincubated either with GST-p115 fusion protein or GST transferred to nitrocellulose strips. The nonbound fractions were tested for inhibitory activity in the semi-intact transport assay. As shown in Fig. 5 B, lane 3, preincubation of the antibody with GST-p115 nitrocellulose strips efficiently neutralized its inhibitory effect on traffic, and processing of VSV-G protein to the endo-H–resistant form was comparable to the control situation with complete cytosol (lane 2). In contrast, inhibition was still apparent with antibodies incubated with GST strips (lane 4), and processing of VSV-G protein to the endo-H–resistant form was comparable to that in the absence of ATP (lane 1). These results suggest that anti–p115 antibodies block ER to Golgi transport through a specific interaction with p115.

To extend these findings, VSV-G protein transport in the presence of limiting amounts of p115 was analyzed. In the semi-intact cell transport assay, exogenous rat liver cytosol must be added to provide cytosolic and peripheral membrane proteins released during permeabilization (Beckers et al., 1987). p115 is peripherally associated with membranes, and during cell disruption, is largely released into the cytosol (Waters et al., 1992; Nelson et al., 1998). Rat liver cytosol contains high amounts of p115 (~0.5 μg/mg). To examine if such exogenously added p115 is required for transport, p115 was removed from the cytosol by immunodepletion. The extent of immunodepletion was analyzed by immunoblotting (Fig. 5 C, p115 panel, lanes 2 and 3 compared with lane 4). The immunoblot was evaluated by densitometry, and the relative amount of p115 present is shown in the accompanying bar graph. Up to 60% of cytosolic p115 was removed in lane 4. When such p115-depleted cytosol was used in the transport assay, VSV-G protein processing to the endo-H–resistant form was inhibited by ~90%. Immunodepletion of cytosol with nonspecific antibodies (affinity-purified rabbit anti–goat IgG, lane 3) or preimmune serum (data not shown) had no effect on VSV-G protein transport. Reactions containing complete transport cocktail (lane 2) or cocktail containing an ATP-depleting system (lane 1) were analyzed as positive and negative controls and defined as 100 and 0% VSV-G protein processing, respectively.

To examine if addition of purified p115 could rescue transport, p115-depleted cytosol (analogous to that in lane 4) was supplemented with increasing amounts of purified p115. p115 was purified from rat liver cytosol on affinity-purified anti–p115 antibodies cross-linked to a protein A–Sepharose column. As shown in Fig. 5 D, the material eluted from the anti–p115 IgG column (lane 1) contains a

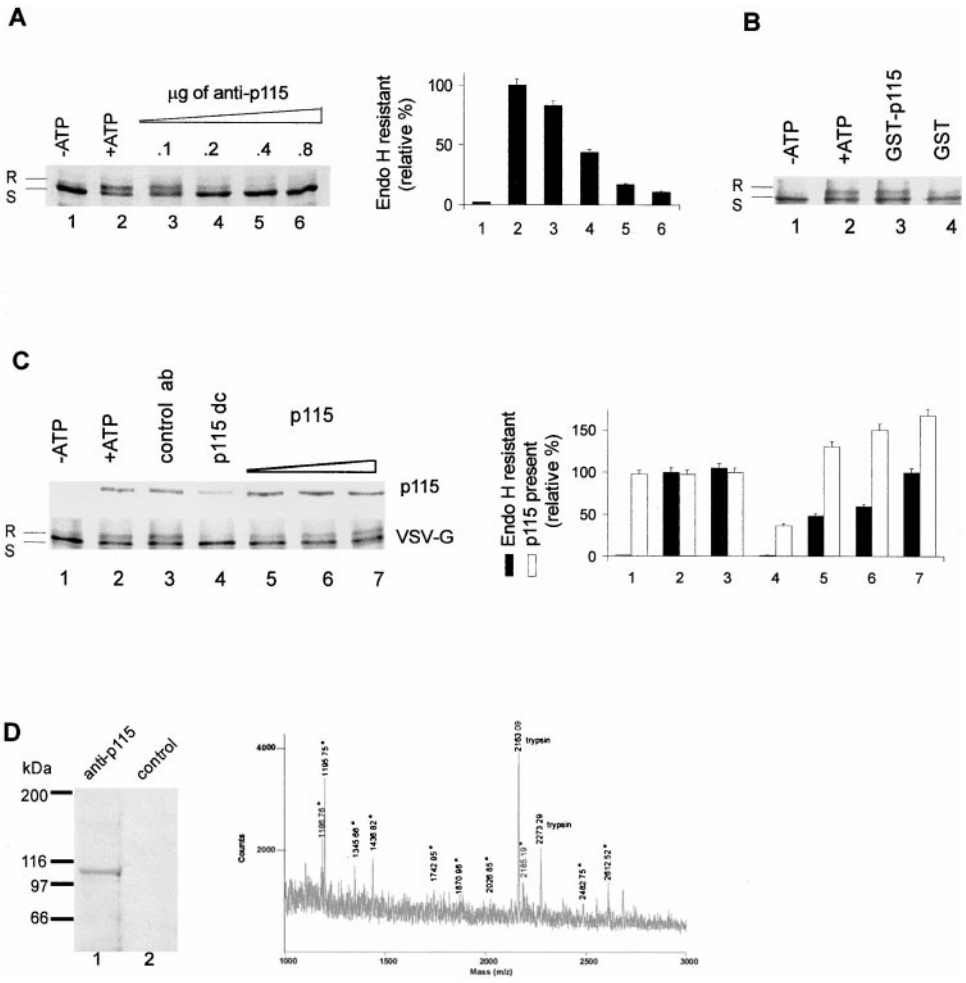

Figure 5. p115 is essential for ER to Golgi transport. ER to Golgi transport was performed in semi-intact NRK cells. Transport is measured as the percentage of VSV-G protein processed from the endo-H–sensitive (S) to the endo-H–resistant (R) form. (A) Transport reactions contained complete transport cocktail (lanes 2–6), or cocktail with ATP-depleting system (lane 1). Reactions were supplemented with increasing amounts of affinity-purified anti–p115 antibodies (lanes 3–6). Transport of VSV-G protein was proportionally inhibited in the presence of antibodies against p115. Analogous gels (n = 3) were quantitated by densitometry and the averages are presented in the bar graph. Transport in lane 1 is set as 0% and in lane 2 as 100%. (B) Transport reactions contained complete transport cocktail (lane 2), cocktail with ATP-depleting system (lane 1), or cocktail supplemented with anti–p115 antibodies preincubated with GST-p115 (lane 3), or GST (lane 4). Preincubation of anti–p115 antibodies with GST-p115 neutralized their inhibitory effect on transport. (C) Transport reactions contained complete transport cocktail (lanes 2–7), or cocktail with ATP-depleting system (lane 1). In lane 3, transport cocktail contained cytosol preincubated with control IgGs. In lane 4, transport cocktail contained cytosol preincubated with anti–p115 antibodies. Reduced level of p115 is visible in lane 4 and leads to inhibition of VSV-G protein transport. Increasing amounts of purified p115 were added to the cytosol shown in lane 4. Addition of purified p115 overcame the inhibitory effect of p115 removal and supported VSV-G protein transport (lanes 5–7). Analogous gels (n = 3) were quantitated by densitometry, and the averages are presented in the bar graph. Transport in lane 1 is set as 0% and in lane 2 as 100%. An aliquot of each transport reaction was probed by immunoblotting with anti–p115 antibodies and the immunoblot is shown in panel p115. The same amount of p115 was used in lane 1 as in lane 2 and only reaction in lane 2 was analyzed. (D) Rat liver cytosol was incubated with anti–p115 antibodies or control IgGs cross-linked to protein A–Sepharose. Bound material was eluted and analyzed by SDS-PAGE. An ~110-kD band was visible after Coomassie blue staining in material eluted from anti-p115 column (lane 1) but not in control eluate (lane 2). The ~110-kD band was excised, digested with trypsin, and the resulting peptides analyzed by MALDI mass spectrometry. The peptide mass map of the 10 most abundant peptides (marked by asterisks) matched the sequence of p115.

band of ~110 kD, whereas no such band was eluted from a control preimmune IgG column (lane 2). To ensure that the 110-kD band was p115, the 110-kD region was excised from a gel, subjected to tryptic digestion and the peptides were separated and characterized by MALDI mass spectrometry combined with sequence database searching. The peptide mass map of 10 major peptides (Fig. 5 D) match with p115, and no other rat protein in that molecular mass range was found in the search. Analogous purified p115 was added to the p115 depleted cytosol. As shown in Fig. 5 C, p115 panel, lanes 5–7, and bar graph, the supplemented cytosol contained 110, ~140, and ~160% of p115 in untreated cytosol, respectively. When such supplemented cytosols were used in the transport assay, VSV-G protein was processed to the endo-H–resistant form with ~40, ~50, and ~100% processing efficiency, respectively (VSV-G panel, lanes 5–7, and bar graph). Taken together, these results indicate that p115 is essential for VSV-G protein delivery from the ER to the Golgi.

p115 Is Required for ER to Golgi Transport at a Step after the rab1 Requirement and before the Ca^{2+} Requirement

Previous work suggested that p115 functions to tether donor and acceptor membranes before membrane fusion (Barroso et al., 1995; Sönnischen et al., 1998), but did not place the p115 requirement relative to requirements for other known transport factors. Studies on Uso1p suggested that its function is regulated by Ypt1p (Sapperstein

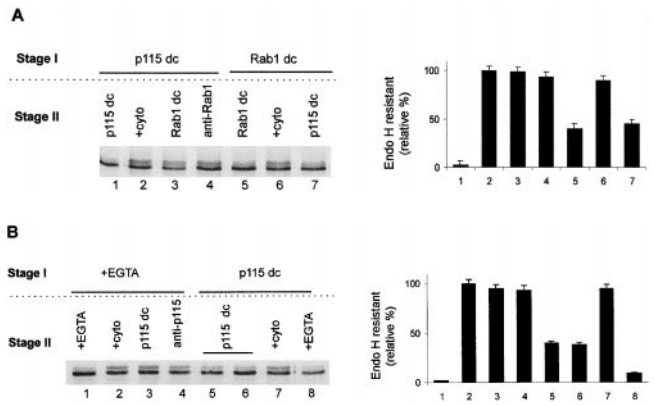

Figure 6. p115 acts after the rab1 requirement and before the Ca^{2+} requirement. Two-stage ER to Golgi transport was performed in semi-intact NRK cells. In stage I, cells were incubated for 60 min at 32°C. Cells were then pelleted and resuspended in fresh transport cocktail and incubated in stage II for 45 min at 32°C. Transport is measured as the percentage of VSV-G protein processed from the endo-H–sensitive (S) to the endo-H–resistant (R) form. (A) VSV-G protein is minimally processed when p115-depleted cytosol is used in both stages (lane 1), and this is set as 0% relative processing. VSV-G protein is processed when complete cytosol (lane 2) is used, and this is set as 100% relative processing. VSV-G protein is processed when rab1-depleted cytosol (lane 3) or cytosol containing anti–rab1 antibodies (lane 4) is added during the second stage. VSV-G protein is not processed when rab1-depleted cytosol is used in both stages (lane 5), but is processed when complete cytosol is used in the second stage (lane 6). VSV-G protein is not processed when p115-depleted cytosol is added during the second stage (lane 7). The staging indicates that p115 acts after the rab1-requiring step of transport. (B) VSV-G protein is minimally processed when EGTA is added to both stages (lane 1), and this is set as 0% relative processing. VSV-G protein is processed when complete transport cocktail is used in both stages (lane 2), and this is set as 100% relative processing. VSV-G protein is processed when p115-depleted cytosol (lane 3) or anti–p115 antibodies (lane 4) are added during the second stage. VSV-G protein is not processed when p115-depleted cytosol is added to both stages (lanes 5 and 6) or when EGTA is added to the second stage (lane 8), but is processed when complete cytosol is added to the second stage (lane 7). The staging indicates that p115 precedes the Ca^{2+}-requiring step of transport.

et al., 1996; Cao et al., 1998), and Ypt1p and its mammalian homologue rab1 are essential for ER to Golgi transport (Plutner et al., 1990, 1991; Schwaninger et al., 1992b; Ferro-Novick and Jahn, 1994; Nuoffer et al., 1994). To order the sequence of rab1- and p115-requiring transport steps in mammalian cells, staging experiments were performed. In the first stage, p115-depleted cytosol was added to the semi-intact cell transport assay, and the cells were incubated at the permissive temperature for 60 min to allow VSV-G protein to accumulate in the p115-arrested compartment. The cells were collected, and in the second stage, incubated with either p115-depleted cytosol, complete cytosol, rab1-depleted cytosol, or complete cytosol supplemented with anti–rab1 antibodies. Rab1-depleted cytosol contained <5% of the rab1 found in untreated cytosol (data not shown), and 3 μg of anti–rab antibodies were used, an amount similar to that shown previously to be inhibitory in the semi-intact cell transport assay (Plutner et al., 1991). As shown in Fig. 6 A (gel and bar graph, lane 1), when p115-depleted cytosol was used in both stages of the transport assay, <10% of VSV-G protein was processed to the endo-H–resistant form. This represents the background of the assay and is set as 0% relative processing. When complete cytosol (lane 2) was added in the second stage, ~35% of VSV-G protein was transported to the Golgi and acquired endo-H resistance (set as 100% relative processing), the same extent as when completed cytosol was used in both stages (data not shown). Significantly, when rab1-depleted cytosol (lane 3), or complete cytosol containing anti–rab1 antibodies (lane 4) were used, comparable ~90% level of relative processing was observed, indicating that progression of VSV-G protein from the p115–depletion blocked compartment to the Golgi does not require rab1.

In agreement with previous results showing partial inhibition after rab1 depletion (Peter et al., 1998), when stages I and II were performed with rab1-depleted cytosol, VSV-G transport was blocked by ~60% (lane 5). When complete cytosol was added in the second stage (lane 6), VSV-G protein processing was >80% of that in lane 2. In contrast, when p115-depleted cytosol was added in the second stage (lane 7), VSV-G protein processing was inhibited by ~60%, the same extent as when rab1-depleted cytosol was used in both stages (lane 5). This suggests that movement of VSV-G protein from the rab1–depletion blocked compartment to the Golgi requires p115. Together, the data indicate that rab1 is required before the p115-requiring step of VSV-G protein transport.

Using the same ER to Golgi transport assay, it has been shown that Ca^{2+} is required at a last transport step before membrane fusion (Beckers and Balch, 1989; Aridor et al., 1995). To determine if addition of anti–p115 antibodies or p115 depletion inhibits ER to Golgi transport at a stage before or after the Ca^{2+} requirement, staging experiments were performed. In the first stage, 10 mM EGTA was added to the semi-intact cell transport assay, and the cells were incubated at the permissive temperature for 60 min to allow VSV-G protein to accumulate in the EGTA-arrested compartment. The cells were collected, and in the second stage, incubated with either cytosol containing 10 mM EGTA, complete cytosol, p115-depleted cytosol, or complete cytosol supplemented with anti–p115 antibodies. As shown in Fig. 6 B (gel and bar graph, lane 1), when EGTA was added to both stages of the transport assay, ~3% of VSV-G protein acquired endo-H resistance. This represents the background of the assay and is set as 0% relative transport. When complete cytosol (lane 2) was added in the second stage, ~35% of VSV-G protein was processed, and this represents 100% relative processing. The ~35% processing is analogous to the percent processing observed when complete cytosol is added to both stages of transport (data not shown). Significantly, when p115-depleted cytosol (lane 3), or complete cytosol containing p115 antibodies (lane 4) was added in the second stage, ~100% relative processing was observed, suggesting that progression of VSV-G protein from the Ca^{2+}-arrested compartment to the Golgi does not require p115.

This was confirmed by reverse staging. As shown in Fig. 6 B (lanes 5 and 6), addition of p115-depleted cytosol to both stages of the transport assay resulted in ~15% of

VSV-G protein acquiring endo-H resistance (~40% relative processing). (In these experiments, p115 depletion was incomplete [data not shown] and accounts for the incomplete inhibition of VSV-G protein transport.) When complete cytosol was added in the second stage (lane 7), ~30% of VSV-G protein was processed (~90% relative processing). When cytosol containing EGTA was added in the second stage, ~5% of the VSV-G protein was transported to the Golgi and acquired endo-H resistance (~10% relative processing) (lane 8). This suggests that movement of VSV-G protein from the p115–depletion blocked compartment to the Golgi stack requires Ca^{2+}. Together, the results indicate that p115 is required before the Ca^{2+}-requiring stage of VSV-G protein transport.

Morphological examination of VSV-G protein localization in the presence of EGTA suggests that Ca^{2+} is required for VTC delivery to the Golgi stack (Aridor et al., 1995). Our finding that p115 is required at a stage of transport before the Ca^{2+} requirement suggested that p115 might also be required at that stage.

p115 Is Required for a VTC Step before the Delivery of VSV-G Protein to the Golgi Stack

To define where anti–p115 antibodies and p115 depletion blocked transport of VSV-G protein, morphological transport assays were performed. Addition of anti–p115 antibodies (~10 ng IgG/μl transport assay, an amount analogous to that shown to inhibit the biochemical assay in Fig. 5 A, lane 5) to the morphological transport assay prevented VSV-G protein from moving to the Golgi (Fig. 7, A–C). A representative experiment (from >10 analyses) is presented. VSV-G protein was not detected in the ER, indicating that anti–p115 antibodies had no effect on VSV-G protein exit from the ER and its delivery to post-ER transport intermediates, but prevented delivery of such intermediates to the Golgi. This resulted in accumulation of VSV-G protein in peripheral VTCs, most of which were labeled with anti–p115 antibodies (C, arrowheads). Anti–p115 antibodies were also detected in the Golgi (C, arrows), perhaps because of incomplete removal of p115

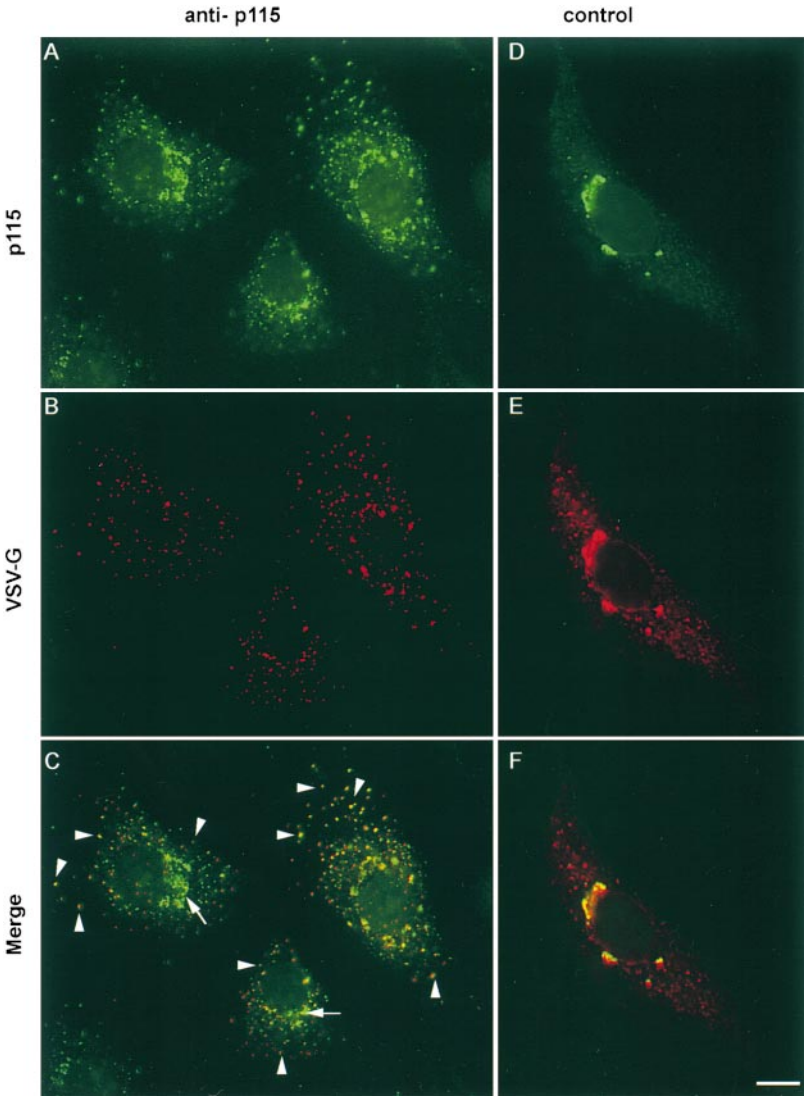

Figure 7. Antibodies against p115 block ER to Golgi transport of VSV-G protein at a pre-Golgi stage. NRK cells were infected with VSVtsO45 for 3 h at 42°C. Cells were permeabilized and supplemented with complete transport cocktail supplemented either with anti–p115 antibodies (A–C) or control antibodies (D–F). After transport at 32°C for 90 min, cells were processed by double label immunofluorescence using anti-p115 (A and D) and anti–VSV-G protein (B and E) antibodies. Addition of anti–p115 antibodies to the transport assay has no effect on VSV-G protein exit from the ER, but prevents VSV-G protein transport to the Golgi (A–C) and causes accumulation of VSV-G protein in scattered VTCs. Arrowheads point to peripheral structures containing VSV-G protein and anti–p115 antibodies. Arrows indicate Golgi elements labeled with anti–p115 antibodies but lacking VSV-G protein. Addition of control antibodies to the transport assay had no effect on VSV-G protein transport, and VSV-G protein was efficiently delivered to the Golgi (D–F). Bar 10 μm.

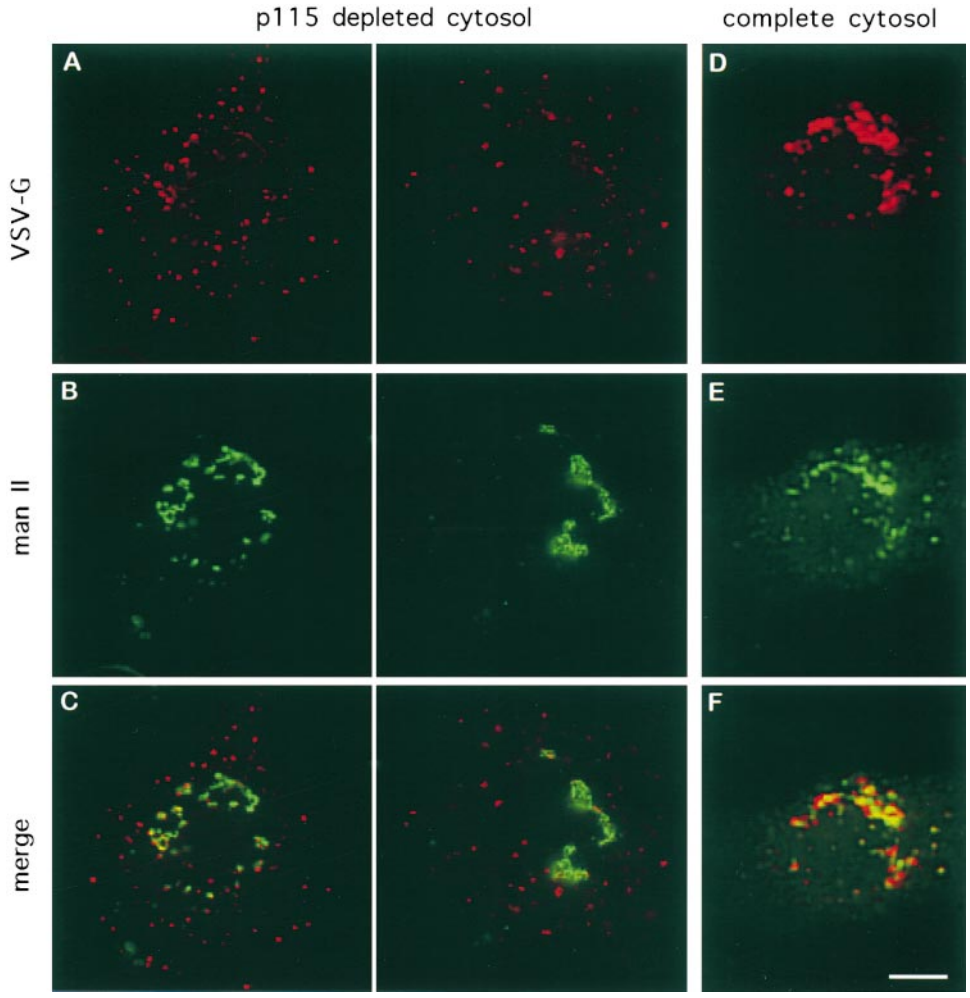

Figure 8. p115 depletion blocks ER to Golgi transport of VSV-G protein at a pre-Golgi stage. NRK cells were infected with VSVtsO45 for 3 h at 42°C. Cells were permeabilized and supplemented with transport cocktails containing p115-depleted cytosol (A–C) or complete cytosol (D–F). After transport at 32°C for 90 min, cells were processed by double label immunofluorescence using anti–VSV-G protein (A and D) and anti–Mann II (B and E) antibodies. Depletion of p115 from the transport assay had no effect on VSV-G protein exit from the ER, but prevented VSV-G protein transport to the Golgi (A–C) and caused accumulation of VSV-G protein in peripheral VTCs lacking Mann II. In the presence of complete cytosol, VSV-G protein was efficiently delivered to the Golgi (D–F). Bar 10 μm.

from membranes during permeabilization. Alternatively, anti–p115 antibodies might act by trapping p115 on Golgi membranes through the formation of inactive complexes. Addition of equivalent amounts of preimmune antibodies to the transport assay had no effect on VSV-G protein transport, and VSV-G protein was efficiently delivered to the Golgi, where it colocalized with p115 (D–F). The same pattern was observed when monoclonal anti–Mann II antibodies were added to the reaction (data not shown).

When p115-depleted cytosol (analogous to that unable to support the biochemical assay in Fig. 5 C, lane 4) was used in the morphological transport assay, VSV-G protein was also not transported to the Golgi, as evidenced by its lack of colocalization with Mann II (Fig. 8, A–C). Two representative cells from two different experiments are shown in these panels. VSV-G protein localized predominantly to peripheral VTCs, indistinguishable from those seen in the presence of anti–p115 antibodies (compare to Fig. 7 B). VSV-G protein was almost exclusively in peripheral VTCs, and was not present to any significant extent in the ER, confirming that p115 is not involved in ER exit and delivery of cargo to more distal transport intermediates. VSV-G protein was efficiently transported to the Golgi when complete cytosol was used (Fig. 8, D–F). Taken together, these results indicate that p115 function is required after the formation of post-ER VTCs but before their delivery to the Golgi stack. This defines a novel function for p115, and identifies the first step of membrane transport in which p115 participates.

Differential Processing of Arrested VSV-G Protein

Since addition of anti–p115 antibodies or p115 depletion inhibits VSV-G protein delivery to the Golgi and causes its accumulation in peripheral VTCs, we expected that the arrested VSV-G protein will not be processed by any of the Golgi glycosyl-modifying enzymes. In agreement, our data show that the arrested VSV-G protein remains endo-H sensitive, indicating a lack of processing by NAGT-1 and Mann II. To examine whether the arrested VSV-G protein is processed by the cis-Golgi enzyme Mann I, endo-D resistance/sensitivity was analyzed in LEC-1 and NRK cells.

Mutant LEC-1 cells that lack NAGT-1 were used first because in these cells oligosaccharide modifications stop after Mann I processing (Stanley et al., 1975). VSV-G protein is endo-D resistant while in the ER and becomes endo-D sensitive after being transported and processed by Mann I. When infected cells were permeabilized and used in the semi-intact cell transport assay in the presence of an

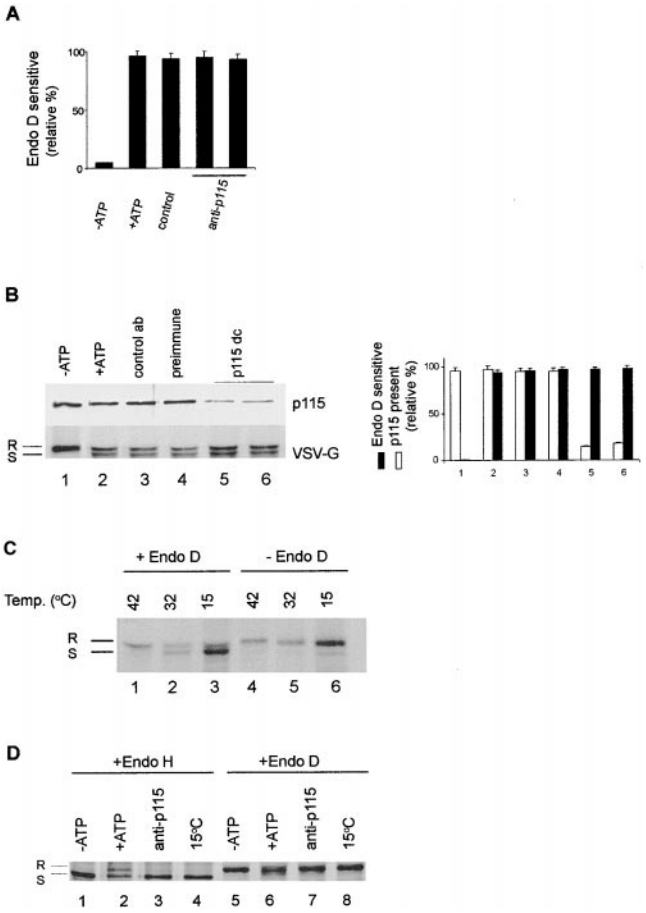

Figure 9. VSV-G protein is differentially endo-D resistant/sensitive in LEC-1 and NRK cells. (A and B) ER to Golgi transport was performed in semi-intact LEC-1 cells. After transport, the sensitivity/resistance of VSV-G protein to endo-D was analyzed. (A) VSV-G protein is endo-D resistant when transport cocktail lacking ATP is used (−ATP), and this is set as 0% relative processing. A proportion of VSV-G protein is endo-D sensitive when complete transport cocktail is used (+ATP), and this is set as 100% relative processing. A similar proportion of VSV-G protein is endo-D sensitive when complete transport cocktails containing control antibodies (control) or anti–p115 antibodies (anti-p115) are used. (B) VSV-G protein is endo-D resistant when transport cocktail lacking ATP is used (lane 1), and this is set as 0% relative processing. A proportion of VSV-G protein is endo-D sensitive when complete transport cocktail is used (lane 2), and this is set as 100% relative processing. A similar proportion of VSV-G protein is endo-D sensitive when complete transport cocktails containing cytosol immunodepleted with control antibodies (lane 3), preimmune antibodies (lane 4), or anti–p115 antibodies (lanes 5 and 6) are used. Analogous gels (n = 3) were quantitated by densitometry and averages are presented as a bar graph. An aliquot of each transport reaction was probed by immunoblotting with anti–p115 antibodies and the immunoblot is shown in panel p115. The relative amounts of p115 in each transport reaction are presented in the bar graph. The amount of p115 in lane 1 is set as 100%. (C) LEC-1 cells were infected with VSVtsO45 for 3 h at 42°C, and either analyzed directly or incubated at 32°C for additional 1 h or at 15°C for additional 3 h before analysis. Cells were collected and analyzed directly or after endo-D digestion. Processing of VSV-G protein from the endo-D–resistant (R) to the endo-D–sensitive (S) form is shown. A single VSV-G band is seen in untreated samples regardless of incubation temperature (lanes 4–6). VSV-G is resistant to endo-D when retained in the ER during the 42°C incubation (lane 1), but becomes endo-D sensitive when transported to the Golgi during a 32°C incubation (lane 2) or when arrested in peripheral VTCs during a 15°C incubation (lane 3). (D, lanes 1–3 and 5–7) ER to Golgi transport was performed in semi-intact NRK cells. After transport, the sensitivity/resistance of VSV-G protein to endo-H and endo-D was analyzed in parallel. VSV-G protein is endo-H sensitive (lane 1) and endo-D resistant (lane 5) when transport cocktail lacking ATP is used. VSV-G protein is endo-H resistant (lane 2) and endo-D resistant (lane 6) when complete transport cocktail is used. VSV-G protein is endo-H sensitive (lane 3) and endo-D resistant (lane 7) when complete transport cocktails containing anti–p115 antibodies are used. (D, lanes 4 and 8) NRK cells were infected with VSVtsO45 (3 h at 32°C), pulsed-labeled at the restrictive temperature (10 min at 42°C) and chased in complete medium for 3 h at 15°C. Cells were collected and digested with either endo-H (lane 4) or endo-D (lane 8). VSV-G protein is endo-H sensitive and endo-D resistant when arrested in peripheral VTCs at 15°C.

ATP-depleting system, VSV-G protein was endo-D resistant (Fig. 9 A, −ATP). When complete transport cocktail was used, a proportion (∼60%) of VSV-G protein became endo-D sensitive, and this is taken as the standard to which other reactions are compared (Fig. 9 A, +ATP). Unexpectedly, VSV-G protein was processed to the endo-D–sensitive form when anti–p115 antibodies were added to the transport assay (Fig. 9 A, anti-p115) in an amount analogous to that found to block acquisition of endo-H resistance in NRK cells (Fig. 5 A, lane 6). Addition of control antibodies had no effect on VSV-G protein processing (Fig. 9 A, control). Similarly, when p115-depleted cytosol was used in the transport assay, VSV-G protein was processed to the endo-D–sensitive form (Fig. 9 B, gel and bar graph, lanes 5 and 6). Even a significant depletion of p115 (>80% of p115 was depleted in lanes 5 and 6 as compared with lane 2) had no effect on the amount of VSV-G protein sensitive to endo-D. The level of p115 (∼20% of control) that supported the processing to the endo-D–sensitive form in LEC-1 cells was unable to support processing to the endo-H–resistant form in NRK cells (compare Fig. 9 B, lane 6, to Fig. 5 C, lane 4). The level of endo-D processing in reactions containing cytosol immunodepleted with anti–p115 antibodies was similar to that when control (Fig. 9 B, lane 3) or preimmune (Fig. 9 B, lane 4) antibodies were used for immunodepletion.

To test VSV-G protein processing by Mann I while in pre-Golgi transport intermediates, we arrested VSV-G protein transport by incubating the LEC-1 cells at 15°C (Rowe et al., 1998). As shown in Fig. 9 C, VSV-G protein is resistant to endo-D when cells are incubated at 42°C (lanes 1 and 4) and becomes endo-D sensitive when incubated at 32°C (lanes 2 and 5). When cells were incubated at 15°C, ∼70% of VSV-G protein was endo-D sensitive (lanes 3 and 6), suggesting that the VSV-G protein was processed by Mann I.

Analogous experiments were performed in NRK cells, but both endo-H and endo-D resistance/sensitivity of VSV-G protein arrested by various treatments were tested. These digestions were done in parallel since only endo-D sensitivity of an endo-H–sensitive form of VSV-G will define whether VSV-G protein is processed by Mann I

but not NAGT-1 and Mann II. As shown in Fig. 9 D, when transport was performed in the presence of an ATP-depleted transport cocktail, VSV-G protein is endo-H sensitive (lane 1) and endo-D resistant (lane 5). When transport was performed in the presence of a complete transport cocktail, VSV-G becomes endo-H resistant (lane 2) and is endo-D resistant (lane 6). When affinity-purified anti–p115 antibodies were added to the complete transport assay, VSV-G protein is endo-H sensitive (lane 3) and endo-D resistant (lane 7). These results differ from the results of analogous experiments performed in LEC-1 cells (Fig. 9 A), in which addition of affinity-purified anti–p115 antibodies leads to VSV-G protein that is endo-D sensitive.

In an attempt to clarify this difference, we analyzed the endo-H and endo-D sensitivity of VSV-G protein arrested in peripheral VTCs when NRK cells are incubated at 15°C. As shown in Fig. 9 D, lanes 4 and 8, VSV-G protein was endo-H sensitive and endo-D resistant. This result differs from that in LEC-1 cells, where an endo-D–sensitive form was observed after 15°C incubation. Together, the data show that endo-D–sensitive VSV-G protein is seen in LEC-1 cells in the presence of anti–p115 antibodies or when cells are incubated at 15°C, whereas the same treatments of NRK cells result in a VSV-G protein that is endo-D resistant. A likely explanation for this difference is that the lack of p115 requirement in LEC-1 cells is due to incomplete inactivation/removal of endogenous p115 from those cells as opposed to NRK cells. Alternatively, since we observe a difference in VSV-G protein endo-D sensitivity in intact LEC-1 and NRK incubated at 15°C, oligosaccharide processing of VSV-G protein might be different in the two cell lines. Currently, we have no explanation for the different results in LEC-1 and NRK cells, and cannot define whether p115 is required for transport of VSV-G protein into a Mann I–containing compartment.

Mann I Redistributes from the Golgi When ER to Golgi Transport Is Blocked by 15°C Incubation or p115 Depletion

The differences in the biochemical results in LEC-1 and NRK cells prompted us to examine Mann I localization in traffic-arrested NRK cells since all previous morphological analyses (Figs. 4, 7, and 8) have been done in NRK cells. Previous EM immunoperoxidase studies indicated that in NRK cells, Mann II is localized in the medial-cisternae, whereas Mann I is localized in the trans-cisternae and the TGN, and at the light immunofluorescence level, both Mann II and Mann I are concentrated in the Golgi region (Velasco et al., 1993). In agreement, Mann I and II colocalized in the Golgi region in cells incubated at 37°C, although Mann I was also present in a more diffuse non-Golgi pattern (Fig. 10, A–C). Significantly, Mann I redistributed from the Golgi to peripheral punctate structures when cells were incubated at 15°C, whereas Mann II did not show such redistribution (Fig. 10, D–F). To characterize these pre-Golgi elements, VSVtsO45-infected cells were shifted from 40 to 15°C for 3 h, and then processed to localize Mann I and VSV-G protein. As shown in Fig. 10, G–I, Mann I redistributed from the Golgi to peripheral structures, some of which (arrowheads, I) contained VSV-G protein. In contrast, Mann II did not show redistribution (Fig. 10, J–L).

To determine whether Mann I can redistribute to pre-Golgi VTCs arrested by p115 depletion, semi-intact cells incubated with transport assays supplemented with complete cytosol or with p115-depleted cytosol were processed for double label immunofluorescence to localize VSV-G protein and Mann I. As shown in Fig. 10, M–O, when transport was performed with complete cytosol, Mann I was detected in a typical perinuclear Golgi structure, where it colocalized with VSV-G protein. In contrast, when transport was performed with p115-depleted cytosol, Mann I was found colocalizing with peripheral VTCs (Fig. 10, P–R, arrowheads in R point to a VTC-containing VSV-G protein and Mann I). As already shown in Fig. 8, Mann II did not show such relocation. Together, these results indicate that Mann I can cycle to pre-Golgi compartments during cargo transit from the ER to the Golgi. Furthermore, our data show that p115 is not required for events before and including the recycling of Mann I from the Golgi to peripheral compartments, but is essential for the subsequent events leading to delivery of cargo and Mann I to the Golgi.

Discussion

Requirement for p115 in Maintaining Golgi Structure

Functional p115 appears to be required for normal Golgi morphology in intact cells since injection of anti–p115 antibodies into WIF-B cells resulted in the appearance of Golgi fragments scattered throughout the injected cells. This antibody effect appears specific since microinjection of anti–5′-nucleotidase antibodies does not lead to changes in Golgi morphology. Normal Golgi architecture varies in different cells, but seems to be dependent on the balance of incoming and outgoing membrane traffic through the structure. Perturbation of the anterograde or retrograde traffic by various treatments of cells leads to Golgi disruption. Specifically, changes in Golgi morphology were observed in cells overexpressing ADP-ribosylation factor (Dascher and Balch, 1994), injected with rab1a mutant (Wilson et al., 1994), or anti–β-COP antibodies (Pepperkok et al., 1993). Similarly, treatment of cells with BFA (Misumi et al., 1986; Fujiwara et al., 1988; Lippincott-Schwartz et al., 1989), nocodazole (Storrie and Yang, 1998), or okadaic acid (Pryde et al., 1998) has a dramatic effect on Golgi integrity. The exact mechanism of the disruptive action of anti–p115 antibodies on Golgi structure is currently unknown, but it is possible that the antibodies perturb transport pathways between the ER and the Golgi. Specifically, the antibodies could inhibit p115 activity in vivo by blocking p115 interactions with GM130 (Nakamura et al., 1997; Nelson et al., 1998), giantin (Sönnischen et al., 1998), or another, as yet unidentified, protein. Alternatively, anti–p115 antibodies might act by trapping p115 on the membranes through the formation of inactive complexes.

Presence of anti–p115 antibodies in cells did not prevent the redistribution of Mann II to the ER after BFA treatment, but the anti–p115 antibodies prevented the reassem-

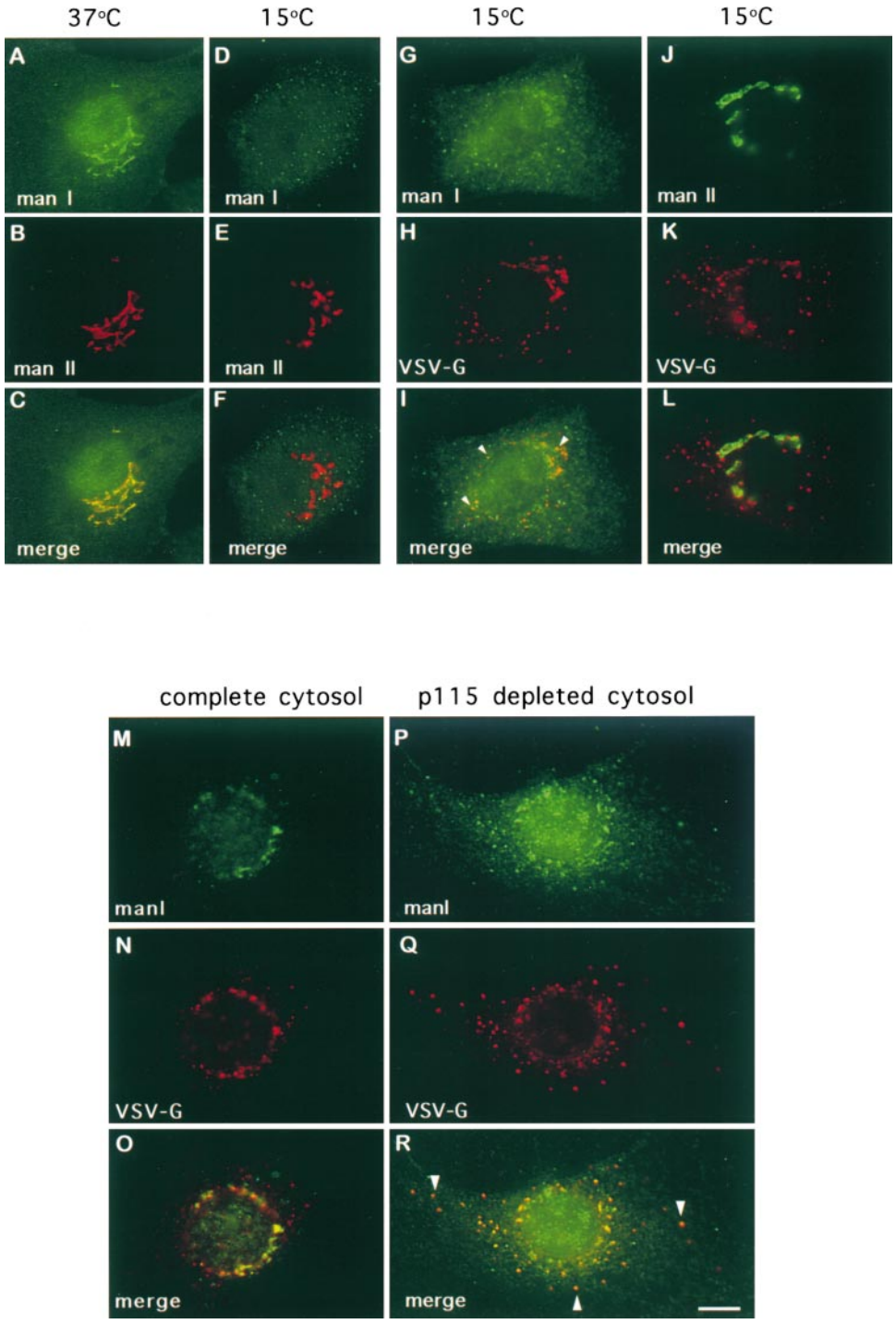

Figure 10. Mann I relocates from the Golgi to arrested pre-Golgi VTCs. NRK cells grown at 37°C (A–C) or incubated for 3 h at 15°C (D–F) were processed for double label immunofluorescence using anti–Mann I (A and D) and anti–Mann II (B and E) antibodies. In cells grown at 37°C, Mann I colocalized with Mann II in the Golgi region (C), but after 15°C incubation, Mann I relocated to peripheral punctate structures and did not colocalize with the Golgi localized Mann II (F). NRK cells infected with VSVtsO45 were incubated for 2 h at 42°C and for an additional 3 h at 15°C (G–L). Cells were processed for double label immunofluorescence using anti–Mann I (G) and anti–VSV-G protein (I) antibodies, or anti–Mann II (J) and anti–VSV-G protein antibodies (K). Mann I is present in dispersed punctate structures, some of which contain VSV-G protein (I, arrowheads). Mann II remains within the Golgi and does not relocate to peripheral structures containing VSV-G protein (L). NRK cells infected with VSVtsO45 were incubated for 3 h at 42°C, permeabilized, and supplemented with transport cocktails containing complete cytosol (M–O) or p115-depleted cytosol (P–R). After transport at 32°C for 90 min, cells were processed for double label immunofluorescence using anti–Mann I (M and P) and anti–VSV-G protein (N and Q) antibodies. In reactions containing complete cytosol, VSV-G protein is delivered to the Golgi where it colocalizes with Mann I (O). In reactions containing p115-depleted cytosol, Mann I relocates to pre-Golgi VTCs containing arrested VSV-G protein (R, arrowheads). Bar, 10 μm.

bly of Golgi complexes during subsequent BFA wash-out. The requirement for functional p115 manifested late, after exit of Golgi enzymes from the ER and delivery to peripherally scattered punctate structures. Significantly, these structures did not move towards the MTOC and did not coalesce into a centrally located Golgi complex. The effect of anti–p115 antibodies was similar to that of anti–EAGE (anti–β-COP) antibodies, which also interfere with the proper reassembly of compact Golgi complexes in a juxtanuclear region during a BFA wash-out (Scheel et al., 1997). Although our findings place the functional requirement for p115 in ER to Golgi traffic between the VTCs and the Golgi, it remains to be determined which step of the anterograde or retrograde transport is blocked by anti–p115 antibodies in vivo.

Requirement for p115 in ER to Golgi Transport

The previous finding that p115 is abundant on VTCs (Nelson et al., 1998) was extended in this study to show that

p115-containing VTCs are functional and carry cargo VSV-G protein from the ER to the Golgi. The possible involvement of p115 in this part of the secretory pathway was examined using previously established ER to Golgi transport assays that measure biochemically or morphologically the movement of VSV-G protein from the ER to the Golgi in semi-intact cells. Our biochemical results show that anti–p115 antibodies or p115 depletion specifically block VSV-G protein transport before acquisition of endo-H resistance, believed to represent the delivery of VSV-G protein to the cis/medial-cisternae of the Golgi stack. Unexpectedly, morphological examination showed that in the presence of anti–p115 antibodies or p115 depletion, VSV-G protein was not delivered to the Golgi stack, but instead was arrested in pre-Golgi peripheral VTCs. These findings indicate that p115 is not required for VSV-G proteins to efficiently exit the ER and be delivered to morphologically normal peripheral VTCs, but is essential for the subsequent delivery of such VTCs to the Golgi stack.

What is the role of p115 in ER to Golgi traffic? Because p115 is predominantly associated with VTCs and p115 depletion arrests transport in VTCs, we favor the hypothesis that p115 functions while on VTCs. A possible role for p115 could be to mediate delivery of essential components from the Golgi to VTCs, by tethering Golgi-derived recycling vesicles to VTCs before fusion. This hypothesis is suggested by the finding that a subpopulation of Golgi-derived COP I vesicles (albeit produced under the nonphysiological conditions of GTPγS treatment) is enriched in giantin, a protein known to bind p115 (Sönnischen et al., 1998). Giantin is an extended coiled-coil transmembrane protein and the interaction between p115 on VTCs and giantin on COP I vesicles could theoretically span the distance of >400 nm, raising the possibility that p115 on VTCs might act to catch and tether giantin-containing Golgi-derived COP I vesicles. Fusion of such vesicles would deliver components essential for VTC maturation and subsequent delivery to the Golgi stack.

Alternatively, p115 might function to mediate VTC motility on microtubules. This is suggested by the fact that the p115-induced block in ER to Golgi traffic is biochemically and morphologically similar to that caused by 15°C incubation, when dynein/dynactin–mediated movement of VTCs on microtubules is inhibited (Presley et al., 1997). Furthermore, VSV-G protein is arrested in peripheral VTCs in cells overexpressing the dynamitin subunit of the dynactin complex (Presley et al., 1997), and their pattern is indistinguishable from VTCs arrested by anti–p115 antibody addition or p115 depletion. Overexpression of dynamitin disrupts the dynactin complex, separating the Arp-1 filament from the dynein-binding arm of $p150^{Glued}$ (Echeverri et al., 1996; Burkhardt et al., 1997) and prevents microtubule-mediated motility. Interestingly, a link between microtubule movement and rab proteins has been established by the finding that the Golgi-localized rab6 interacts with rabkinesin, a Golgi-associated kinesin-like motor protein that binds to microtubules and is likely to mediate membrane movement along microtubules (Echard et al., 1998). Whether rab1 might also have motor proteins (perhaps of the dynein/dynactin family) as one of its effectors remains to be determined. However, it is interesting that p115 structure is similar to that of kinesin (a dimer with globular heads, a central coiled-coil tail, and a tail domain), although p115 does not contain an ATP-binding/hydrolysis domain and does not interact with microtubules (data not shown).

It is equally possible that p115 is required to recruit or activate other uncharacterized factors that will ultimately allow VTC transport and fusion. We do not consider it likely that p115 function in VTC dynamics involves interaction with GM130, since GM130 is not detected on VTCs (Nelson et al., 1998) or Golgi-derived COP I vesicles (Sönnischen et al., 1998), and appears restricted to the Golgi stack. It is more probable that p115–GM130 interactions occur after the VTCs are delivered to the Golgi stack.

Functional p115 was shown to be required in ER to Golgi traffic after the rab1-dependent step of transport. Rab1 has been shown previously to be required after COP II vesicle budding and after the assembly of peripheral VTCs (Peter et al., 1998). In semi-intact cells supplemented with the rab1a (N124I) mutant that is defective for guanine nucleotide binding, VSV-G protein has been shown at the ultrastructural level to accumulate in tubular structures with associated coated vesicular profiles (Pind et al., 1994), but the morphology of the p115-arrested transport intermediates remains to be analyzed. The behavior of p115 and rab1 in mammalian cells is analogous to that of Uso1p and Ypt1 in yeast, since Ypt1p appears to act upstream of Uso1p, and might be indirectly involved in recruiting Uso1p to the membranes (Cao et al., 1998). Whether rab1 performs a similar function for p115 is uncertain since significant differences in the dynamics of transport intermediates (e.g., yeast do not appear to have extensive VTCs) are evident.

p115 was found to act before the Ca^{2+}-requiring step, which is considered to be the last stage of transport before fusion (Aridor et al., 1995). SNARE pairing precedes Ca^{2+} requirement (Chen et al., 1999), and our data are consistent with the reported requirement for Uso1p before SNARE complex formation (Sapperstein et al., 1996; Barlowe, 1997; Cao et al., 1998).

Cycling of Golgi Enzymes to Pre-Golgi Compartments

This report documents the first instance of a morphologically observed relocation of Mann I from the Golgi stack to peripheral pre-Golgi structures. The relocation is apparent in cells in which ER to Golgi transport is blocked by 15°C incubation or p115 depletion, suggesting that Mann I (like other Golgi proteins) cycles between the Golgi and the ER. The mechanism of Golgi protein recycling is largely undefined. Recycling might occur directly from the Golgi to the ER, since direct delivery via tubular structures is observed during BFA-induced relocation of Golgi proteins, and at least one Golgi glycosylating enzyme, GalT, can be detected in similar tubules under physiological conditions (Sciaky et al., 1997). The BFA-induced tubular relocation of Golgi proteins is COP I–independent (Donaldson et al., 1991). Alternatively, recycling might occur from the Golgi to VTCs. This pathway would be consistent with the biochemical data showing that VSV-G protein arrested in pre-Golgi transport intermediates can be processed by NAGT-1, which recycles via small vesicles from the Golgi to the pre-Golgi intermedi-

ates (Love et al., 1998). The recent results showing that NAGT-1 binds coatomer in vitro (Dominguez et al., 1998), and NAGT-1, as well Mann II and Gal-T, bud from the Golgi in COP I–coated vesicles (Lanoix et al., 1999) suggest that COP I–coated vesicles might transport Golgi-derived glycosyl transferases to pre-Golgi transport intermediates. Based on the structural similarity of Mann I to other glycosyltransferases (a type II transmembrane protein), it is possible that it also recycles via Golgi-derived COP I–coated vesicles.

Previous work has defined the kinetics with which Golgi resident proteins cycle between the Golgi and the ER. Several Golgi proteins such as KDEL-R, TGN38 (Cole et al., 1998), and gp27 (Fullekrug et al., 1999), and glycosylating enzymes such as *N*-acetylgalactosaminyltransferase-2 (GalNAc-T2) and GalT (Storrie et al., 1998) have been shown to cycle with half lives between 20 min (e.g., the KDEL-R; Cole et al., 1998) and 2–3 h (e.g., gp27 [Fullekrug et al., 1999]; GalNAc-T2 and GalT [Storrie et al., 1998]). Based on our observation that the majority of Mann I relocates from the Golgi and appears in blocked VTCs during a 90-min incubation at 37°C (the time course of the semi-intact transport assay), it appears that Mann I cycles with relatively fast kinetics. Although the semi-intact cell system used in our studies is not designed to analyze recycling pathways, the results showing relocation of Mann I, but not of Mann II to peripheral VTCs suggests that Mann II cycles with significantly slower kinetics.

The recycling kinetics of Mann I seem more similar to those of the ERGIC proteins, KDEL-R and ERGIC53, which cycle rapidly at 37°C. These proteins also relocate to peripheral VTCs during longer (usually ~3 h) incubations at 15°C. However, Mann I does not appear to be a bonafide component of the ERGIC since EM analysis showed it to be localized throughout the Golgi stack, with highest concentration in the trans-cisternae and the TGN, rather than the cis-face of the stack (Velasco et al., 1993). This suggests that rapid cycling is not restricted to residents of the ERGIC, and that proteins with steady state distribution in more distal Golgi compartments including the TGN, also contain signals for rapid cycling. Whether the recycling mechanisms are the same and involve COP I vesicles, or are distinct remains to be elucidated.

Our morphological results have direct bearing on the controversy regarding the mode of cargo transport through the Golgi. The finding that Mann I efficiently relocates from the Golgi stack to colocalize with peripheral cargo-containing VTCs is less consistent with the anterograde vesicular traffic model than with the maturation model for exocytic traffic. Our results are not consistent with the anterograde vesicular traffic model, in which glycosyl-transferases remain relatively stationary in distinct Golgi cisternae while the cargo is shuttled from proximal to distal cisterna in small vesicles. The observed relocation supports the maturation model, in which cargo progresses through the secretory pathway in a compartment that is remodeled by the sequential recycling of processing enzymes from later Golgi compartments.

We thank Dr. Gerry Waters and Dr. Sandy Harris (both from Princeton University, Princeton, NJ) for providing monoclonal anti–p115 antibodies, Dr. Marilyn Farquhar for providing anti–Mann II antibodies, Dr. Mark McNiven for providing anti–rab1 antibodies, Dr. Kelley Moreman for providing anti–Mann I antibodies, and Dr. Hans-Peter Hauri for providing anti–giantin antibodies. We are grateful to Drs. Joachim Osterman (EMBL, Heidelberg, Germany) and Ellen Tisdale (Wayne State University, Detroit, MI) for critical reading of the manuscript. We also thank Drs. Kathryn Howell and Con Beckers (University of Alabama, Birmingham, AL) for helpful discussions.

References

Aridor, M., S.I. Bannykh, T. Rowe, and W.E. Balch. 1995. Sequential coupling between COPII and COPI vesicle coats in endoplasmic reticulum to Golgi transport. *J. Cell Biol.* 131:875–893.

Aridor, M., J. Weissman, S. Bannykh, C. Nuoffer, and W.E. Balch. 1998. Cargo selection by the COPII budding machinery during export from the ER. *J. Cell Biol*. 141:61–70.

Balch, W.E., M.M. Elliott, and D.S. Keller. 1986. ATP-coupled transport of vesicular stomatitis virus G protein between the endoplasmic reticulum and the Golgi. *J. Biol. Chem*. 261:14681–14689.

Balch, W.E., J.M. McCaffery, H. Plutner, and M.G. Farquhar. 1994. Vesicular stomatitis virus glycoprotein is sorted and concentrated during export from the endoplasmic reticulum. *Cell*. 76:841–852.

Bannykh, I., and W. Balch. 1997. Membrane dynamics at the endoplasmic reticulum–Golgi interface. *J. Cell Biol.* 138:1–4.

Bannykh, S.I., T. Rowe, and W.E. Balch. 1996. The organization of endoplasmic reticulum export complexes. *J. Cell Biol*. 135:19–35.

Bannykh, S.I., N. Nishimura, and W. Balch. 1998. Getting into the Golgi. *Trends Cell Biol*. 8:21–25.

Barlowe, C. 1997. Coupled ER to Golgi transport reconstituted with purified cytosolic proteins. *J. Cell Biol.* 139:1097–1108.

Barlowe, C. 1998. COPII and selective export from the endoplasmic reticulum. *Biochem. Biophys. Acta.* 1404:67–76.

Barroso, M., D. Nelson, and E. Sztul. 1995. Transcytosis-associated protein (TAP)/p115 is a general fusion factor required for binding of vesicles to acceptor membranes. *Proc. Natl. Acad. Sci. USA*. 92:527–533.

Beckers, C.J., and W.E. Balch. 1989. Calcium and GTP: essential components in vesicular trafficking between the endoplasmic reticulum and Golgi apparatus. *J. Cell Biol.* 108:1245–1256.

Beckers, C.J., D.S. Keller, and W.E. Balch. 1987. Semi-intact cells permeable to macromolecules: use in reconstitution of protein transport from the endoplasmic reticulum to the Golgi complex. *Cell*. 50:523–534.

Bergmann, J. 1989. Using temperature-sensitive mutants of VSV to study membrane protein biogenesis. *Methods Enzymol.* 32:85–110.

Burkhardt, J.K., C.J. Echeverri, T. Nilsson, and R.B. Vallee. 1997. Overexpression of the dynamitin (p50) subunit of the dynactin complex disrupts dynein-dependent maintenance of membrane organelle distribution. *J. Cell Biol.* 139:469–484.

Cao, X., N. Ballew, and C. Barlowe. 1998. Initial docking of ER-derived vesicles requires Uso1p and Ypt1p but is independent of SNARE proteins. *EMBO (Eur. Mol. Biol. Organ.) J.* 17:2156–2165.

Chavrier, P., R.G. Parton, H.-P. Hauri, K. Simons, and M. Zerial. 1990. Localization of low molecular weight GTP binding proteins to exocytic and endocytic compartments. *Cell*. 62:317–329.

Chen, Y.A., S.J. Scales, S.M. Patel, Y.-C. Doung, and R.H. Scheller. 1999. SNARE complex formation is triggered by Ca^{2+} and drives membrane fusion. *J. Cell Biol.* 97:165–174.

Cole, N.B., J. Ellenberg, J. Song, D. DiEuliis, and J. Lippincott-Schwartz. 1998. Retrograde transport of Golgi-localized proteins to the ER. *J. Cell Biol.* 140: 1–15.

Dascher, C., and W.E. Balch. 1994. Dominant inhibitory mutants of ARF1 block endoplasmic reticulum to Golgi transport and trigger disassembly of the Golgi apparatus. *J. Biol. Chem*. 269:1437–1448.

Dascher, C., J. Matteson, and W.E. Balch. 1994. Syntaxin 5 regulates endoplasmic reticulum to Golgi transport. *J. Biol. Chem*. 269:29363–29366.

Dominguez, M., K. Dejgaard, J. Fullekrug, S. Dahan, A. Fazel, J. Paccaud, T.Y. Thomas, J.J.M. Bergeron, and T. Nilsson. 1998. gp25L/emp24/p24 protein family members of the cis-Golgi network bind both COP I and II coatomer. *J. Cell Biol*. 140:751–765.

Donaldson, J.G., J. Lippincott-Schwartz, and R.D. Klausner. 1991. Guanine nucleotides modulate the effects of brefeldin A in semipermeable cells: regulation of the association of 110-kD peripheral membrane protein with the Golgi apparatus. *J. Cell Biol*. 112:579–588.

Donaldson, J.G., D. Cassel, R.A. Kahn, and R.D. Klausner. 1992a. ADP-ribosylation factor, a small GTP-binding protein, is required for binding of the coatomer protein β-COP to Golgi membranes. *Proc. Natl. Acad. Sci. USA*. 89:6408–6412.

Donaldson, J.G., D. Finazzi, and R.D. Klausner. 1992b. Brefeldin A inhibits Golgi membrane-catalysed exchange of guanine nucleotide onto ARF protein. *Nature*. 360:350–352.

Echard, A., F. Jollivet, O. Martinez, J.J. Lacapere, A. Rousselet, I. Janoueix-Lerosey, and B. Goud. 1998. Interaction of a Golgi-associated kinesin-like protein with Rab6. *Science*. 279:580–585.

Echeverri, C.J., B.M. Paschal, K.T. Vaughan, and R.B. Vallee. 1996. Molecular characterization of the 50-kD subunit of dynactin reveals function for the

complex in chromosome alignment and spindle organization during mitosis. *J. Cell Biol.* 132:617–633.
Ferro-Novick, S., and R. Jahn. 1994. Vesicle fusion from yeast to man. *Nature.* 370:191–193.
Fujiwara, T., K. Oda, S. Yokota, A. Takatsuki, and Y. Ikehara. 1988. Brefeldin A causes disassembly of the Golgi complex and accumulation of secretory proteins in the endoplasmic reticulum. *J. Biol. Chem.* 263:18545–18552.
Fullekrug, J., T. Suganuma, B.L. Tang, W. Hong, B. Storrie, and T. Nilsson. 1999. Localization and recycling of gp27 (hp24γ3): complex formation with other p24 family members. *Mol. Biol. Cell.* 10:1939–1955.
Glick, B.S., and V. Malhotra. 1998. The curious status of the Golgi apparatus. *Cell.* 95:883–889.
Hanson, P.I., R. Roth, H. Morisaki, R. Jahn, and J.E. Heuser. 1997. Structure and conformational changes in NSF and its membrane receptor complexes visualized by quick-freeze/deep-etch electron microscopy. *Cell.* 90:523–535.
Hay, J.C., and R.H. Scheller. 1997. SNAREs and NSF in targeted membrane fusion. *Curr. Opin. Cell Biol.* 9:505–512.
Helms, J.B., and J.E. Rothman. 1992. Inhibition by brefeldin A of a Golgi membrane enzyme that catalyses exchange of guanine nucleotide bound to ARF. *Nature.* 360:352–354.
Hong, W. 1998. Protein transport from the endoplasmic reticulum to the Golgi apparatus. *J. Cell Sci.* 111:2831–2839.
Klausner, R.D., J.G. Donaldson, and J. Lippincott-Schwartz. 1992. Brefeldin A: insights into the control of membrane traffic and organelle structure. *J. Cell Biol.* 116:1071–1080.
Ladinsky, M.S., D.N. Mastronarde, J.R. McIntosh, K.E. Howell, and L.A. Staehelin. 1999. Golgi structure in three dimensions: functional insights from the normal rat kidney. *J. Cell Biol.* 144:11–35.
Lanoix, J., J. Ouwendijk, C. Lin, A. Stark, H.D. Love, J. Osterman, and T. Nilsson. 1999. GTP hydrolysis by arf-1 mediates sorting and concentration of Golgi resident enzymes into functions COP I vesicles. *EMBO (Eur. Mol. Biol. Organ.) J.* 18:4935–4948.
Linstedt, A.D., and H.-P. Hauri. 1993. Giantin, a novel conserved Golgi membrane protein containing a cytoplasmic domain of at least 350 kDa. *Mol. Biol. Cell.* 4:679–693.
Lippincott-Schwartz, J. 1998. Cytoskeletal proteins and Golgi dynamics. *Curr. Opin. Cell Biol.* 10:52–59.
Lippincott-Schwartz, J., L.C. Yuan, J.S. Bonifacino, and R.D. Klausner. 1989. Rapid redistribution of Golgi proteins into the ER in cells treated with brefeldin A: evidence for membrane cycling from Golgi to ER. *Cell.* 56:801–813.
Lippincott-Schwartz, J., J.G. Donaldson, A. Schweizer, E.G. Berger, H.-P. Hauri, L.C. Yuan, and R.D. Klausner. 1990. Microtubule-dependent retrograde transport of proteins into the ER in the presence of brefeldin A suggests an ER recycling pathway. *Cell.* 60:821–836.
Love, H.D., C.C. Lin, C.S. Short, and J. Ostermann. 1998. Isolation of functional Golgi-derived vesicles with a possible role in retrograde transport. *J. Cell Biol.* 140:541–551.
Lowe, M., and T.E. Kreis. 1998. Regulation of membrane traffic in animal cells by COPI. *Biochem. Biophys. Acta.* 1404:53–66.
McNew, J.A., M. Sogaard, N.M. Lampen, S. Machida, R.R. Ye, L. Lacomis, P. Tempst, J.E. Rothman, and T.H. Söllner. 1997. Ykt6p, a prenylated SNARE essential for endoplasmic reticulum-Golgi transport. *J. Biol. Chem.* 272: 17776–17783.
Misumi, Y., Y. Misumi, K. Miki, A. Takatsuki, G. Tamura, and Y. Ikehara. 1986. Novel blockade by brefeldin A of intracellular transport of secretory proteins in cultured rat hepatocytes. *J. Biol. Chem.* 261:1398–1403.
Nakajima, H., A. Hirata, Y. Ogawa, T. Yonehara, K. Yoda, and M.A. Yamasaki. 1991. Cytoskeleton-related gene, uso1, is required for intracellular protein transport in *Saccharomyces cerevisiae*. *J. Cell Biol.* 113:245–260.
Nakamura, N., M. Lowe, T.P. Levine, C. Rabouille, and G. Warren. 1997. The vesicle docking protein p115 binds GM130, a cis-Golgi matrix protein, in a mitotically regulated manner. *Cell.* 89:445–455.
Nelson, D., C. Alvarez, Y. Gao, R. García-Mata, E. Fialkowski, and E. Sztul. 1998. The membrane transport factor TAP/p115 cycles between the Golgi and earlier secretory compartments and contains distinct domains required for its localization and function. *J. Cell Biol.* 143:319–331.
Nichols, B.J., and H.R. Pelham. 1998. SNAREs and membrane fusion in the Golgi apparatus. *Biochem. Biophys. Acta.* 1404:9–31.
Nuoffer, C., H.W. Davidson, J. Matteson, J. Meinkoth, and W.E. Balch. 1994. A GDP-bound of rab1 inhibits protein export from the endoplasmic reticulum and transport between Golgi compartments. *J. Cell Biol.* 125:225–237.
Orci, L., A. Perrelet, and J.E. Rothman. 1998. Vesicles on strings: morphological evidence for processive transport within the Golgi stack. *Proc. Natl. Acad. Sci. USA.* 95:2279–2283.
Pepperkok, R., J. Scheel, H. Horstmann, H.-P. Hauri, G. Griffiths, and T.E. Kreis. 1993. Beta-COP is essential for biosynthetic membrane transport from the endoplasmic reticulum to the Golgi complex in vivo. *Cell.* 74:71–82.
Peter, F., H. Plutner, H. Zhu, T.E. Kreis, and W.E. Balch. 1993. β-COP is essential for transport of protein from the endoplasmic reticulum to the Golgi in vitro. *J. Cell Biol.* 122:1155–1167.
Peter, F., S.H. Wong, V.N. Subramaniam, B.L. Tang, and W.J. Hong. 1998. α-Snap but not γ-snap is required for ER-Golgi transport after vesicle budding and the rab1-requiring step but before the EGTA-sensitive step. *J. Cell Sci.* 111:2625–2633.
Pfeffer, S.R. 1996. Transport vesicle docking: SNAREs and associates. *Annu. Rev. Cell Dev. Biol.* 12:441–461.
Pind, S.N., C. Nuoffer, J.M. McCaffery, H. Plutner, H.W. Davidson, M.G. Farquhar, and W.E. Balch. 1994. Rab1 and Ca^{2+} are required for the fusion of carrier vesicles mediating endoplasmic reticulum to Golgi transport. *J. Cell Biol.* 125:239–252.
Plutner, H., R. Schwaninger, S. Pind, and W.E. Balch. 1990. Synthetic peptides of the Rab effector domain inhibit vesicular transport through the secretory pathway. *EMBO (Eur. Mol. Biol. Organ.) J.* 9:2375–2383.
Plutner, H., A.D. Cox, S. Pind, R. Khosravi-Far, J.R. Bourne, R. Schwaninger, C.J. Der, and W.E. Balch. 1991. Rab1b regulates vesicular transport between the endoplasmic reticulum and successive Golgi compartments. *J. Cell Biol.* 115:31–43.
Plutner, H., H.W. Davidson, J. Saraste, and W.E. Balch. 1992. Morphological analysis of protein transport from the ER to Golgi membranes in digitonin-permeabilized cells: role of the P58 containing compartment. *J. Cell Biol.* 119:1097–1116.
Presley, J.F., N.B. Cole, T.A. Schroer, K. Hirschberg, J.M. Zaal, and J. Lippincott-Schwartz. 1997. ER-to-Golgi transport visualized in living cells. *Nature.* 389:81–85.
Pryde, J.G., T. Farmaki, and J.M. Lucocq. 1998. Okadaic acid induces selective arrest of protein transport in the rough endoplasmic reticulum and prevents export into COPII-coated structures. *Mol. Cell Biol.* 18:1125–1135.
Rabouille, C., T.R. Misteli, R. Watson, and G. Warren. 1995. Reassembly of Golgi stacks from mitotic Golgi fragments in a cell-free system. *J. Cell Biol.* 129:605–618.
Rabouille, C., H. Kondo, R. Newman, N. Hui, P. Freemont, and G. Warren. 1998. Syntaxin 5 is a common component of the NSF- and p97-mediated reassembly pathways of Golgi cisternae from mitotic Golgi fragments in vitro. *Cell.* 92:603–610.
Rothman, J.E. 1994. Mechanisms of intracellular protein transport. *Nature.* 372: 55–63.
Rowe, T., C. Dascher, S. Bannykh, H. Plutner, and W.E. Balch. 1998. Role of vesicle-associated syntaxin 5 in the assembly of pre-Golgi intermediates. *Science.* 279:696–700.
Sapperstein, S.K., D.M. Walter, A.R. Grosvenor, J.E. Heuser, and M.G. Waters. 1995. p115 is a general vesicular transport factor related to the yeast endoplasmic reticulum to Golgi transport factor Uso1p. *Proc. Natl. Acad. Sci. USA.* 92:522–526.
Sapperstein, S.K., V.V. Lupashin, H.D. Schmitt, and M.G. Waters. 1996. Assembly of the ER to Golgi SNARE complex requires Uso1p. *J. Cell Biol.* 132:755–767.
Saraste, J., and K. Svensson. 1991. Distribution of the intermediate elements operating in ER to Golgi transport. *J. Cell Sci.* 100:415–430.
Scales, S.J., R. Pepperkok, and T.E. Kreis. 1997. Visualization of ER-to-Golgi transport in living cells reveals a sequential mode of action for COPII and COPI. *Cell.* 90:1137–1148.
Scheel, J., R. Pepperkok, M. Lowe, G. Griffiths, and T.E. Kreis. 1997. Dissociation of coatomer from membranes is required for brefeldin A–induced transfer of Golgi enzymes to the endoplasmic reticulum. *J. Cell Biol.* 137: 319–333.
Schwaninger, R., H. Plutner, G.M. Bokoch, and W.E. Balch. 1992a. Multiple GTP-binding proteins regulate vesicular transport from the ER to Golgi membranes. *J. Cell Biol.* 119:1077–1096.
Schwaninger, R., H. Plutner, H.W. Davidson, S. Pind, and W.E. Balch. 1992b. Transport of protein between endoplasmic reticulum and Golgi compartments in semiintact cells. *Methods Enzymol.* 219:110–124.
Schweizer, A., J.A. Fransen, T. Bachi, L. Ginsel, and H.-P. Hauri. 1988. Identification, by a monoclonal antibody, of a 53-kD protein associated with a tubulo-vesicular compartment at the cis-side of the Golgi apparatus. *J. Cell Biol.* 107:1643–1653.
Sciaky, N., J. Presley, C. Smith, K.J.M. Zaal, N. Cole, J.E. Moreira, M. Terasaki, E. Siggia, and J. Lippincott-Schwartz. 1997. Golgi tubule traffic and the effects of brefeldin A visualized in living cells. *J. Cell Biol.* 139:1137–1155.
Segev, J., J. Mulholland, and D. Botstein. 1988. The yeast GTP-binding protein and a mammalian counterpart are associated with the secretion machinery. *Cell.* 52:915–924.
Shanks, M.R., D. Cassio, O. Lecoq, and A.L. Hubbard. 1994. An improved polarized rat hepatoma hybrid cell line. Generation and comparison with its hepatoma relatives and hepatocytes in vivo. *J. Cell Sci.* 107:813–825.
Söllner, T., S.W. Whiteheart, M. Brunner, H. Erdjument-Bromage, S. Geromanos, P. Tempst, and J.E. Rothman. 1993. SNAP receptors implicated in vesicle targeting and fusion. *Nature.* 362:318–324.
Sönnischen, B., M. Lowe, T. Levine, E. Jämsä, B. Dirac-Svejstrup, and G. Warren. 1998. A role for giantin in docking COPI vesicles to Golgi membranes. *J. Cell Biol.* 140:1013–1021.
Stanley, P., S. Narasimhan, L. Siminovitch, and H. Schachter. 1975. Chinese hamster ovary cells selected for resistance to the cytotoxicity of phytohemagglutinin are deficient in a UDP-N-acetylglucosamine–glycoprotein N-acetylglucosaminyltransferase activity. *Proc. Natl. Acad. Sci. USA.* 72: 3323–3327.
Storrie, B., and W. Yang. 1998. Dynamics of the interphase mammalian Golgi complex as revealed through drugs producing reversible Golgi disassembly. *Biochem. Biophys. Acta.* 1404:127–137.
Storrie, B., J. White, S. Rottger, E.H.K. Stelzer, T. Suganuma, and T. Nilsson.

1998. Recycling of Golgi-resident glycosyltransferases through the ER reveals a novel pathway and provides an explanation for nocodazole-induced Golgi scattering. *J. Cell Biol.* 143:1505–1521.

Subramaniam, V.N., F. Peter, R. Philp, S.H. Wong, and W. Hong. 1996. GS28, a 28-kilodalton Golgi SNARE that participates in ER-Golgi transport. *Science*. 272:1161–1163.

Tang, B.L., S.H. Low, H.P. Hauri, and W. Hong. 1995. Segregation of ERGIC53 and the mammalian KDEL receptor upon exit from the 15 degrees C compartment. *Eur. J. Cell Biol.* 68:398–410.

Tisdale, E.J., and W.E. Balch. 1996. Rab2 is essential for the maturation of pre-Golgi intermediates. *J. Biol. Chem*. 271:29372–29379.

Tisdale, E.J., J.R. Bourne, R. Khosravi-Far, C.J. Der, and W.E. Balch. 1992. GTP-binding mutants of rab1 and rab2 are potent inhibitors of vesicular transport from the endoplasmic reticulum to the Golgi complex. *J. Cell Biol.* 119:749–761.

Velasco, A., L. Hendricks, K.W. Moremen, D.R. Tulsiani, O. Touster, and M.G. Farquhar. 1993. Cell type–dependent variations in the subcellular distribution of α-Mann I and II. *J. Cell Biol.* 122:39–51.

Waters, M.G., D.O. Clary, and J.E. Rothman. 1992. A novel 115-kD peripheral membrane protein is required for intercisternal transport in the Golgi stack. *J. Cell Biol.* 118:1015–1026.

Wilson, B.S., C. Nuoffer, J.L. Meinkoth, M. McCaffery, J.R. Feramisco, W.E. Balch, and M.G. Farquhar. 1994. A Rab1 mutant affecting guanine nucleotide exchange promotes disassembly of the Golgi apparatus. *J. Cell Biol.* 125:557–571.

Yamakawa, H., D.H. Seog, K. Yoda, M. Yamasaki, and T. Wakabayashi. 1996. Uso1 protein is a dimer with two globular heads and a long coiled-coil tail. *J. Struct. Biol.* 116:356–365.